VINANST-14
(2021/12/10, Dalat, Vietnam）

大阪府立大学
OSAKA PREFECTURE UNIVERSITY
高度研究型大学～世界に翔く地域の信頼拠点～

HEAT FLUX MONITORING AND CONTROL IN THE NUCLEAR FUSION TECHNOLOGY

Osaka Prefecture University
Radiation Research Center/
Graduate School Eng.
H.Matsuura
M.Akiyoshi

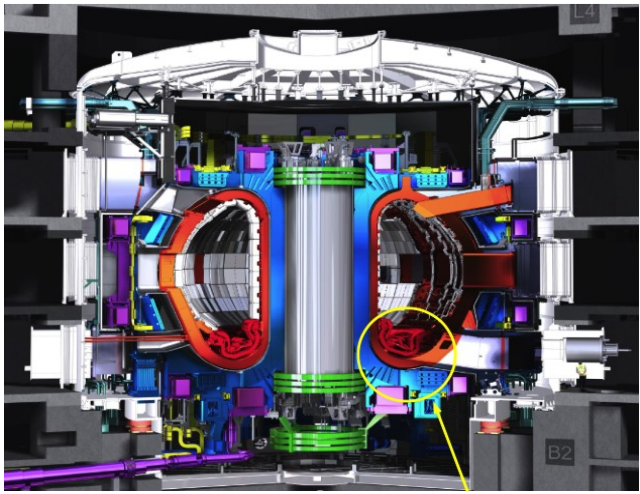

Today's talk contents

- Brief introduction Osaka metropolitan University
- Heat load problem in fusion technology
- Heat conduction model to determine plasma heat flux onto surrounding materials
- Detached plasma formation mechanism and V-shaped target plate effect
- Conclusion

This work is partially performed with the support and under the auspices of the NIFS Collaborative Research Program. (NIFS20KLPR051/ NIFS20KUHL099 / NIFS20KUGM153)

大阪府立大学
OSAKA PREFECTURE UNIVERSITY
高度研究型大学～世界に翔く地域の信頼拠点～

大阪市立大学
OSAKA CITY UNIVERSITY

Osaka Metropolitan University
(Tentative name)

Asahimachi 1-2-7-601, Osaka Abeno-ku, Osaka 545-0051 Japan

Establish approval submission was accepted at September,2021 by Japanese government.

Osaka Metropolitan University
(Tentative name)

Asahimachi 1-2-7-601, Osaka Abeno-ku, Osaka 545-0051 Japan

※Currently applying for establishment approval.
The contents and the organization here are subject to change.

Establish approval submission was accepted at September,2021 by Japanese government.

12 Colleges and 15 Graduate Schools

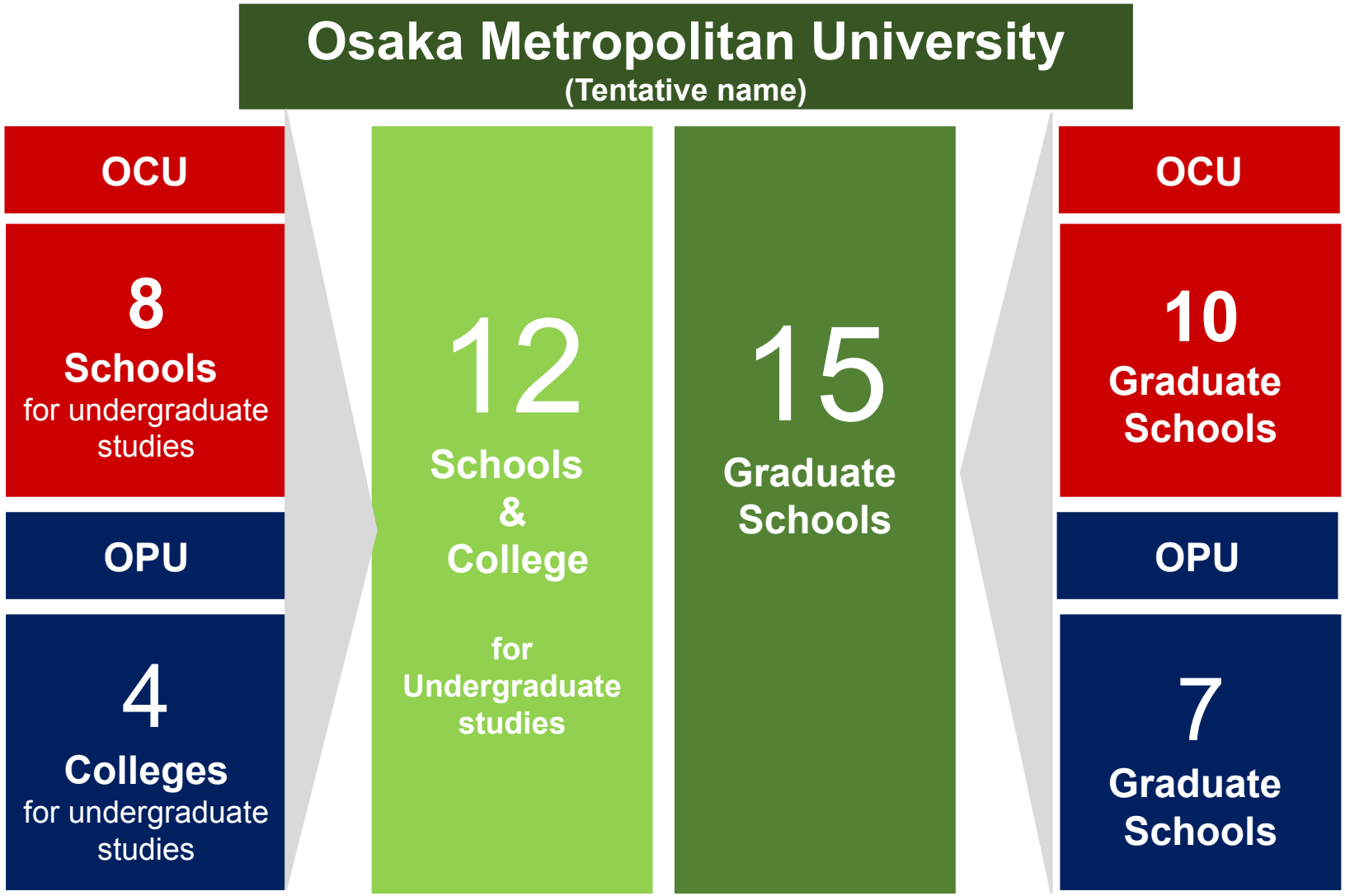

※Currently applying for establishment approval.
The contents and the organization here are subject to change.

Official English website is now available!

※Currently applying for establishment approval.
The contents and the organization here are subject to change.

https://osakamet.jp/

Establish approval submission was accepted at September,2021 by Japanese government.

Division of Quantum and Radiation Engineering

- Established at 2013 and will be celebrated 5th anniversary in this year.
- Contains only one small department (about 10 person/year), and have no undergraduate course.
- Educate people who can manage safely radiation, radio isotope, radiation generator.
- Educate people who can judge risk and benefit of radiation with correct knowledge, and communicate with a wide generation.

Recruit of students

Quantum and Radiation does not have undergraduate school course. So we invite students from

Other undergraduate school
Collage of technology
Other University

Other country (Vietnam, China, Laos, ...)

Even from wide area, we accept new student.
New research will start in our graduate school course.

What is nuclear fusion?

- Energy source of Sun and almost everything on the earth.
- If we can control it on the earth, we get almost eternal energy.
- More than 60 years research was conducted and still many 10 years is necessary.
- Most serious problem is radiation related with tritium fuel and neutron induce activation, and heat control in plasma material interaction.

Natural nuclear fusion reactor

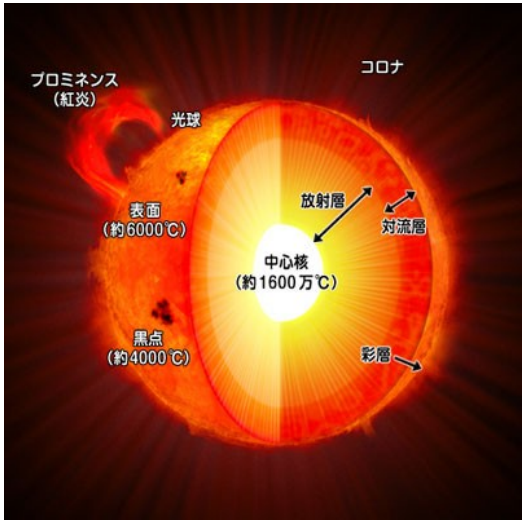

太陽系図鑑
http://rikanet2.jst.go.jp/contents/cp0320a/contents/taiyoukei/taiyou/taiyou_03.html

Reaction rate is very small and power density is smaller than even a human body (~1kW/m^3).
We need much compact reactor.

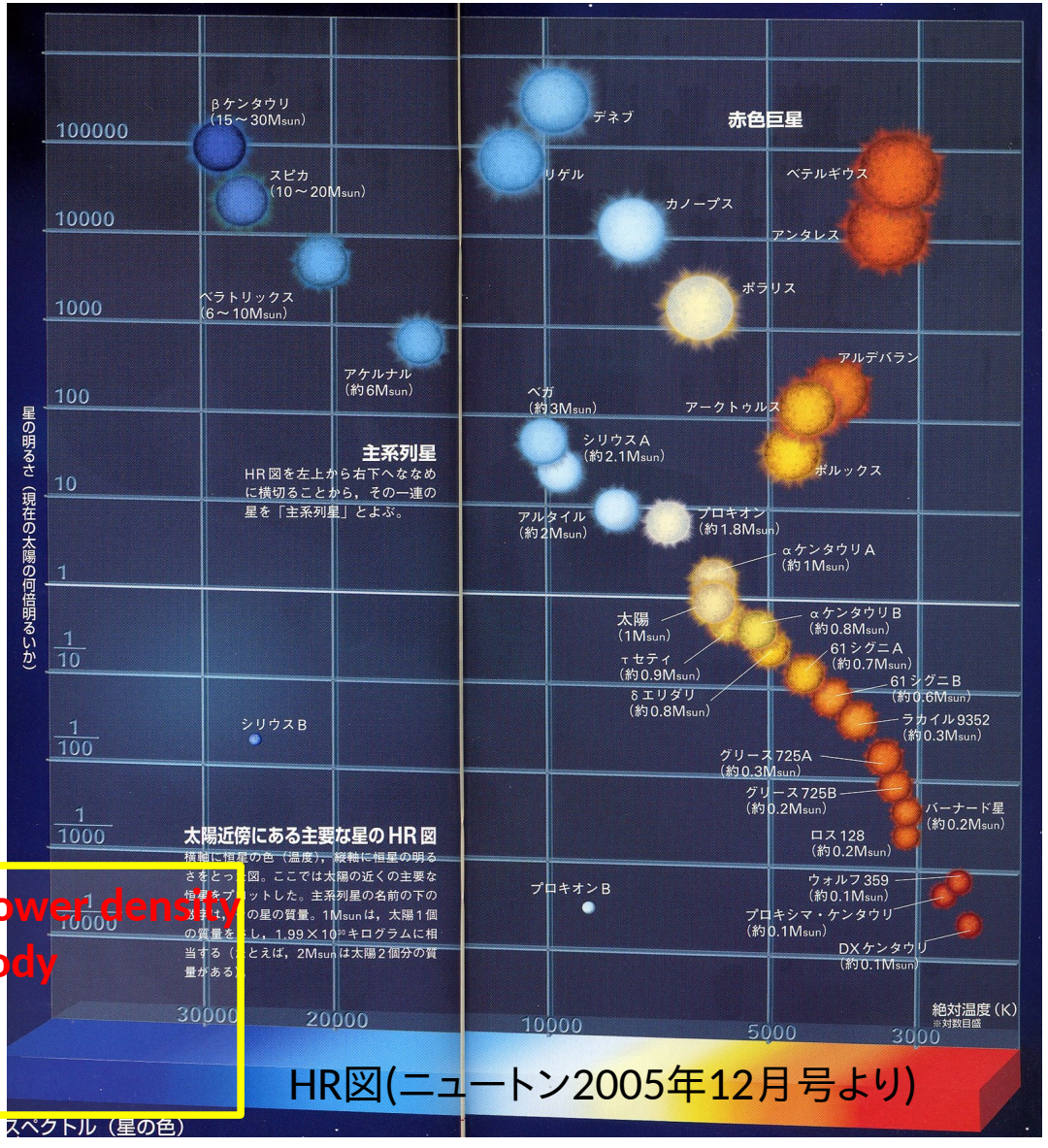

HR図(ニュートン2005年12月号より)

DT nuclear fusion

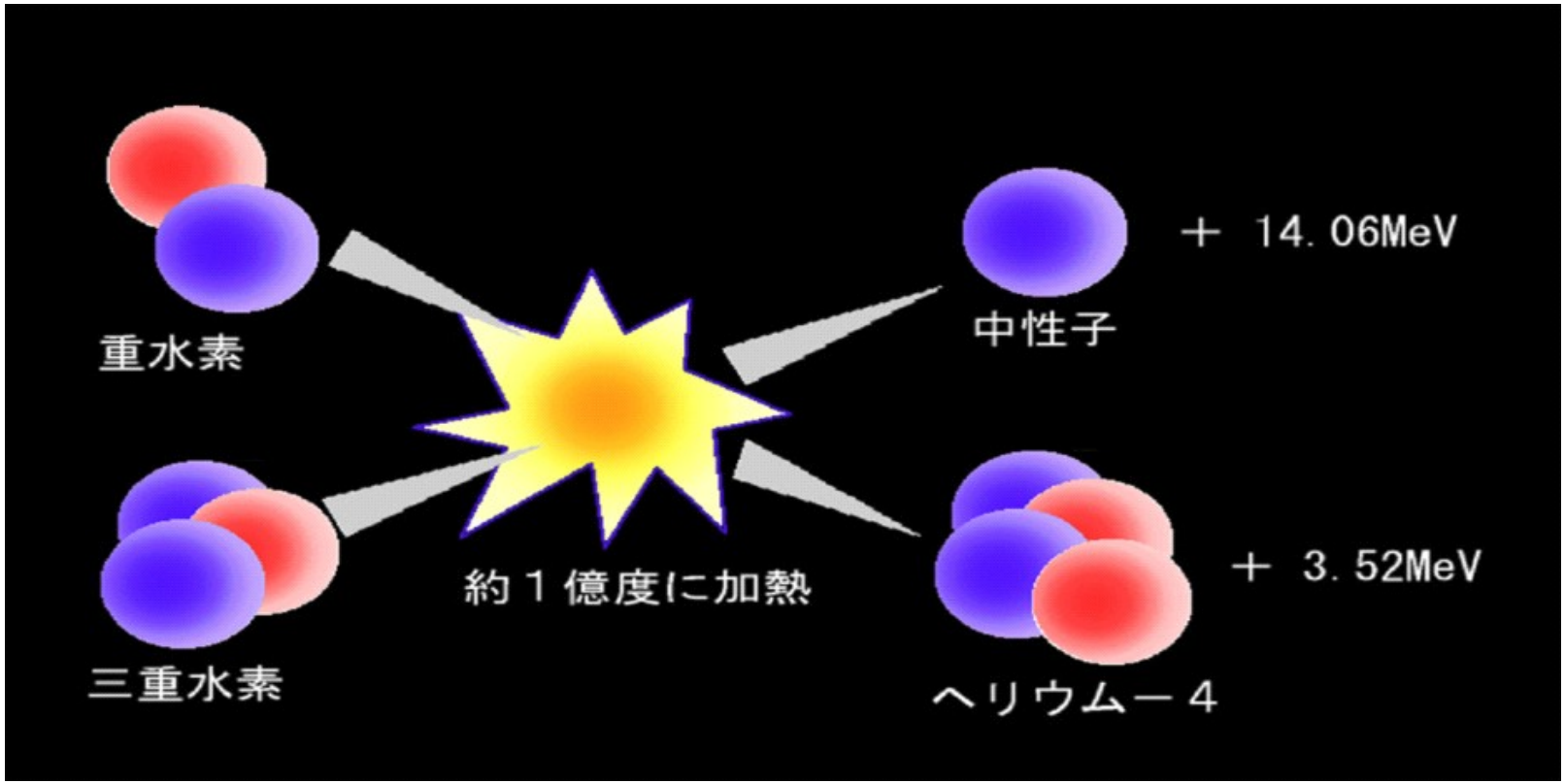

Since weak interaction (beta-decay) does not included, much higher power density can be obtained compared with our sun.
In JET (current largest Tokamak), power density of 100kW/m^3 is obtained in 1990th.

So thermal problem in DT reactor is much harder than Sun.

Divertor

ITER

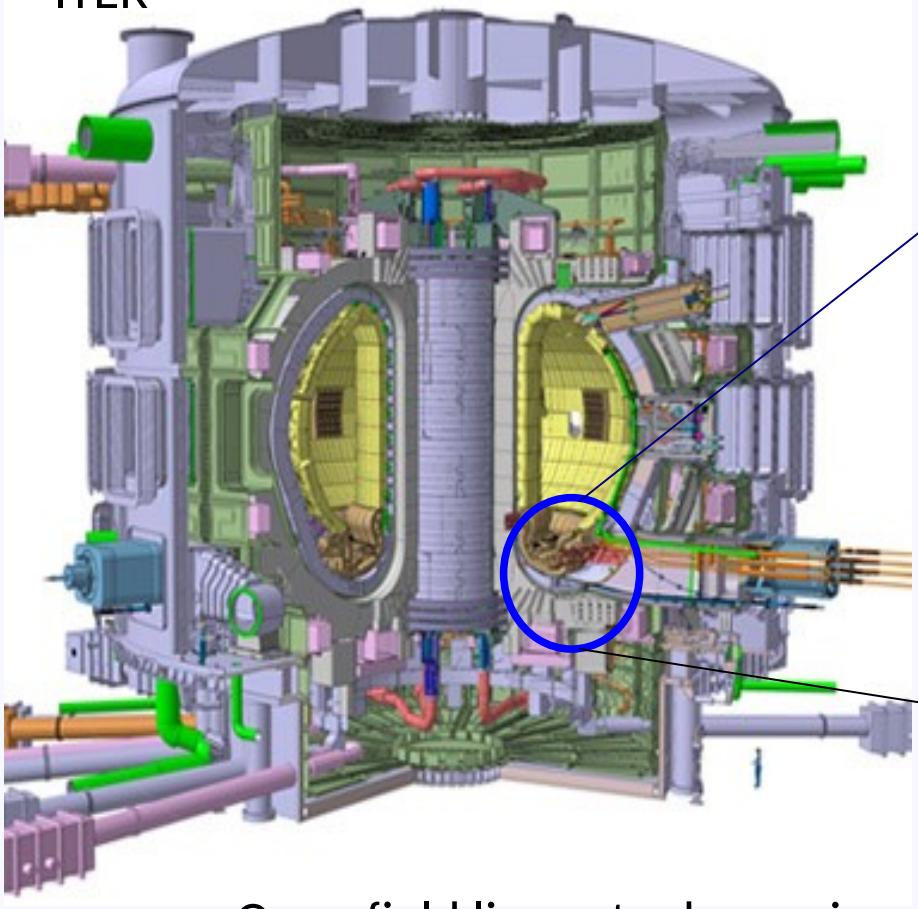

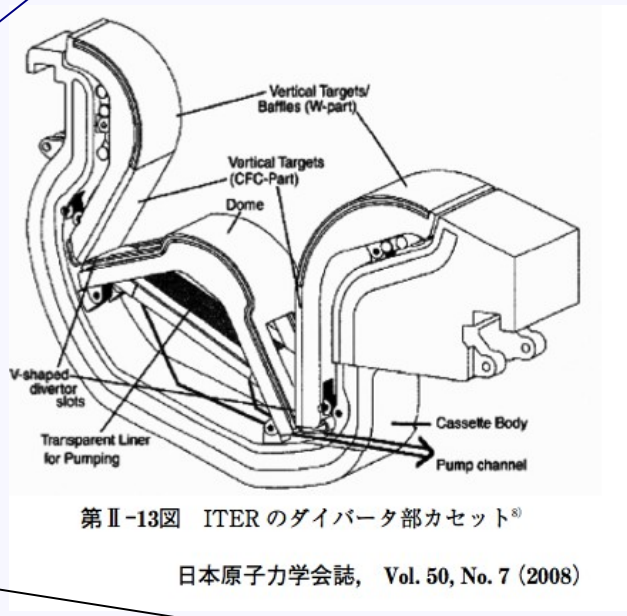

第Ⅱ-13図　ITER のダイバータ部カセット[8)]

日本原子力学会誌，Vol. 50, No. 7 (2008)

Open field lines at edge region of fusion reactor terminate at solid plate,
where heat flux of order of that at sun surface concentrates
and heat control becomes an important issue.

Value of Heat load

	Fusion reactor(ITER)	W/m^2
Solar energy	(Atmospheric plasma)	~10^3
radiator		~10^4
1000K black body	First wall	~10^5
Fuel rod in reactor		~10^6
Rocket engine	Divertor plate	~10^7
Sun surface		~10^8
	Current disruption, ELM	~10^9

How does divertor sustain such huge heat load?

Detachment(Plasma side)
Promoted transport(material side)

Thermal problem in nuclear fusion technology

- Heat load reduction with “Detached plasma” formation

  Exact measurement heat flux

  Understand of molecular activated recombination in detachment formation

- Keeping of cooling ability maximum of divertor plate

  Research on thermal properties degradation under neutron irradiation

Detached plasma(MAP-II)

Steady state hydrogen or helium arc plasma, equivalent to fusion edge plasma, is produced with . LaB6 electrode.

By increasing target chamber pressure, light emission just before target plate is observed to disappear.

Heat flux/heat load estimation

Total fusion reactor system and plasma are not in equilibrium state.

Plasma state can be changed under control or accidentally in short time scale.

Does current heat flux estimation in fusion community really satisfy heat balance?

Is this heat flux estimation rational?

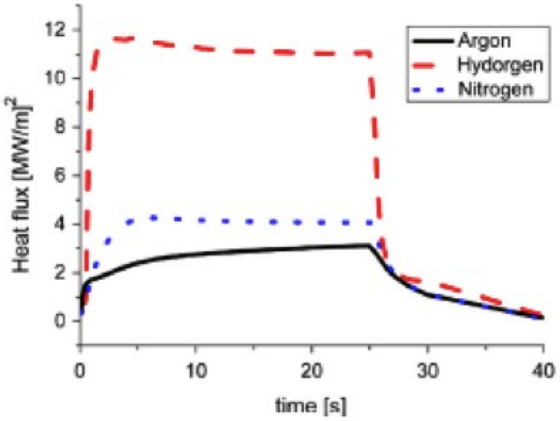

Fig. 1. The heat flux calculated with Ansys from the IR camera temperature and the calorimetry. The upper graph shows the profile at 20 s, the bottom graph shows the maximum heat flux plotted versus time.

Tungsten targets of 1 mm thick and 30 mm in diameter are used, clamped onto a water cooled copper heat sink, with grafoil® in between to ensure a good contact surface [8]. The target was kept at a floating potential. The targets are exposed to the plasma for 25 s with a magnetic field of 0.8 T, TS is done after 20 s. In argon slightly higher source settings can be used; 225 A through the arc with a gas flow of 2.4 slm. In hydrogen and nitrogen the source settings are 200 A with 2 slm.

Why heat flux > 0,
even after irradiation stop

Surface temp. by IR camera
Calorimetry of coolant
are not shown

ANSYS analysis
Boundary condition
are not declared

Keeping heat balance and reproducing temperature evolution are lacking in these similar paper.

Heat balance based on control volume (CV) concept

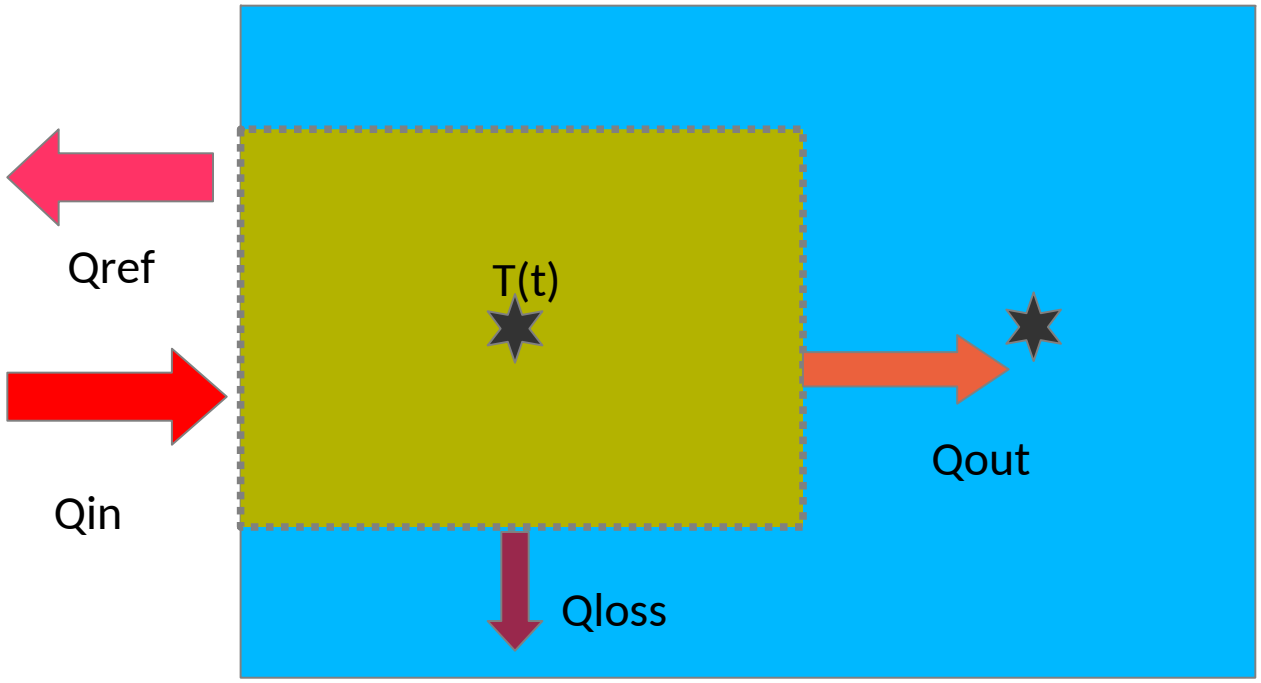

Temperature evolution measured with TC
Is determined by net heat influx through boundary of CV
(and heat generation of inside and boundary of CV).

Control volume heat balance equation

$$c\rho V\frac{dT(t)}{dt} = Q_{in} - Q_{out} - Q_{loss} + S_{vol}$$

Initial condition

$$T = T_0$$

boundary condition (Upside)

$$Q_{plasma} - Q_{rad} + S_{surf} = Q_{in}$$

boundary condition (Downside)

$$Q_{out} = 0(\text{Insulation}) \sim \infty(\text{heatsink})$$

Side effect Q_{loss}

Heat source S_{vol}, S_{surf}

Assignment of control volume(CV)

It is possible ether to set whole heat receiving target as one big CV, nor to divide the target into many small CVs.

When CVs are set on side surface, new boundary conditions must be assigned there.

It is not rational to cover whole first wall with one CV to omit this boundary condition.

Heat flow through boundaries must be modeled with boundary conditions or representative temperature of neighboring CVs.

Temperature gradient method

(Temperature gradient type Thermal Probe)

ref :Osakabe; Rev. Sci. Instrum., Vol. 72, No. 1,(2001)586.

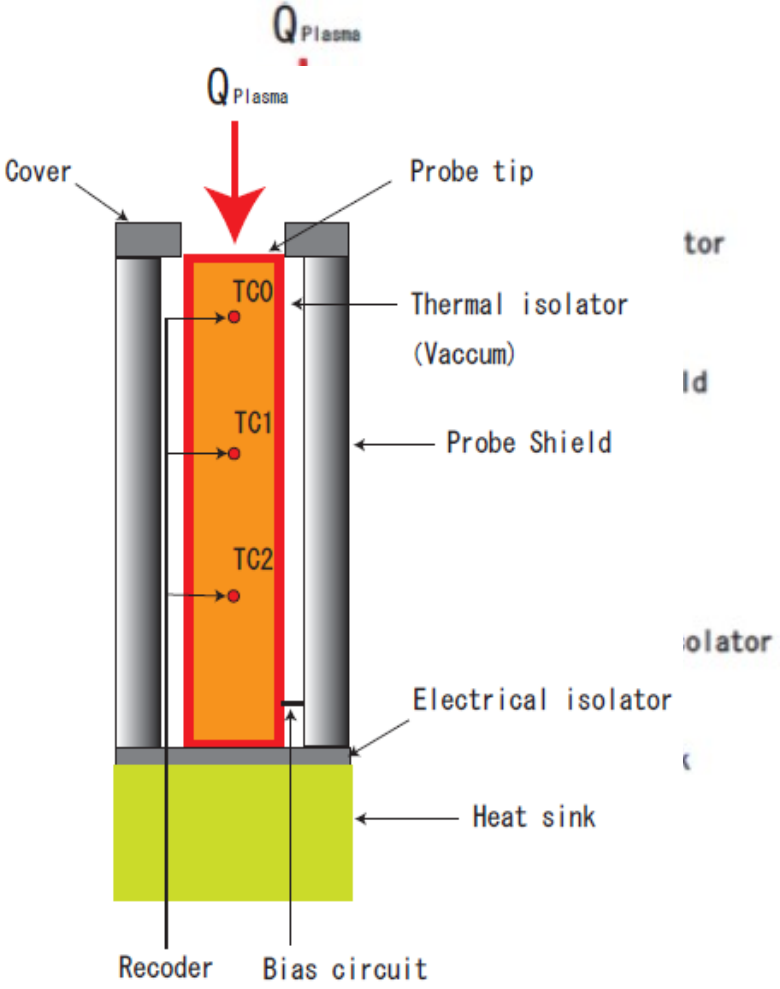

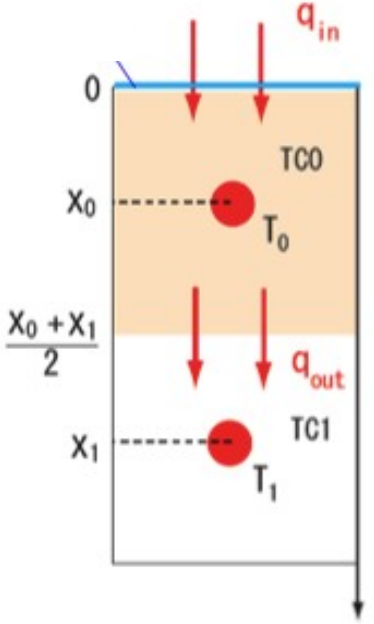

$(0 \sim \frac{x_0 + x_1}{2})$

$$q_{in} = -\kappa \frac{T_1 - T_0}{x_1 - x_0} + \rho c_p \left(\frac{x_0 + x_1}{2} \right) \frac{\partial T_0}{\partial t}$$

Conduction q1 — internal energy q2

Pulse decompose method

H.Matsuura et al., Contrib. Plasma Phys. 54 (2014) 285-290.

Some contribution can be negative.

A pair of positive and negative ones with same amplitude consist a pulse.

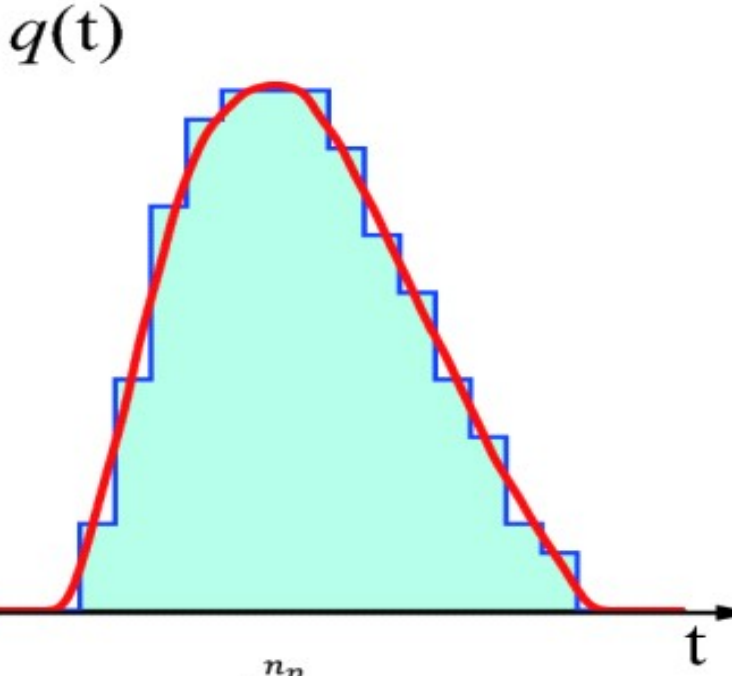

$$q(t) \sim \sum_{i=1}^{n_p} q_0 C_i H(t - t_i)$$

The size of each step C_i is determined so as that the summation of their temperature response reproduces the observed temperature variation data.

$$T(t) - T_0 \sim \sum_{i=1}^{n_p} C_i S_i(t) \qquad (2)$$

Heat step response function

For step-like heat flux

$$q(t) = \begin{cases} 0 & (t < t_i) \\ q_0 & (t > t_i) \end{cases} .$$

temperature response differs according to TC position.

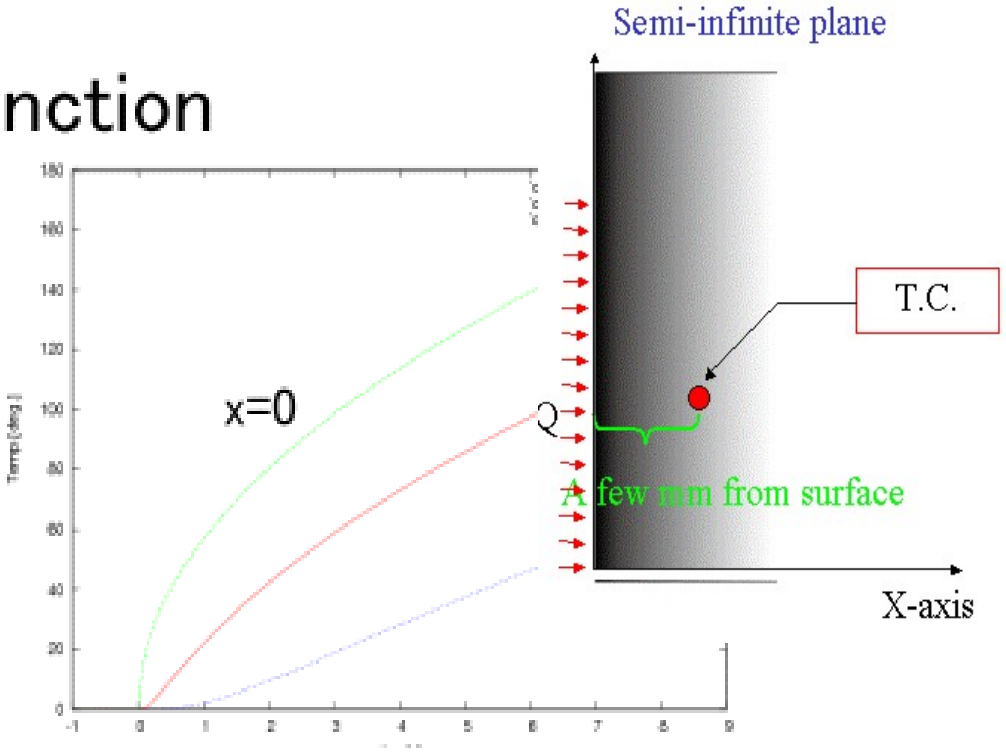

Infinite boundary

When a slab target with thickness of L start to recieve heat flux denisty q_0 at $t = 0$. If L is sufficiently large, temperature response function is given as

$$T(x,t) - T_0 = \Delta T \sqrt{\frac{4\alpha t}{L^2}} \mathrm{ierfc}\left(\frac{x}{\sqrt{4\alpha t}}\right) \tag{1}$$

where $\Delta T = \frac{q_0 L}{\kappa}$, and $\mathrm{ierfc}(x) = -x\mathrm{erfc}(x) + \frac{1}{\sqrt{\pi}} \exp(-x^2)$. x is normalized with L and t is normalized with $\tau = \frac{4L^2}{\pi^2 \alpha}$, where $\alpha = \frac{\kappa}{c\rho}$.

GAMMA10/PDX movable calorimeter system

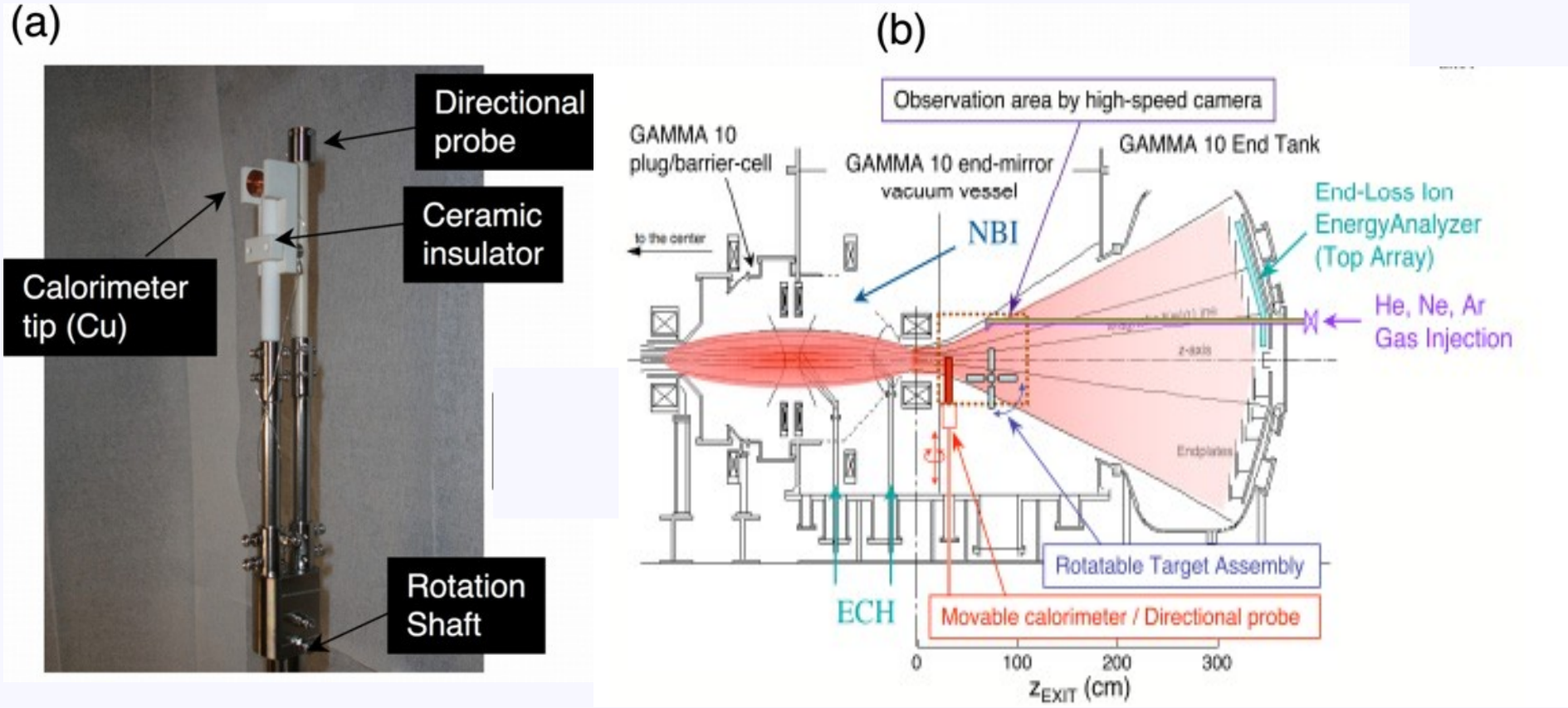

The west end-mirror region, together with the location of the diagnostic equipment installed for this experiment.

New calorimeter target (2016)

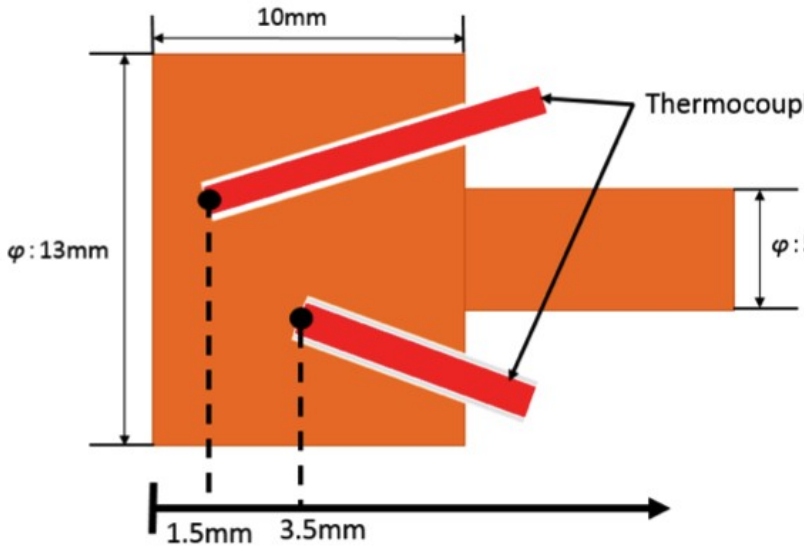

Material of substrate :
cupper
Thermocouple : K - Type

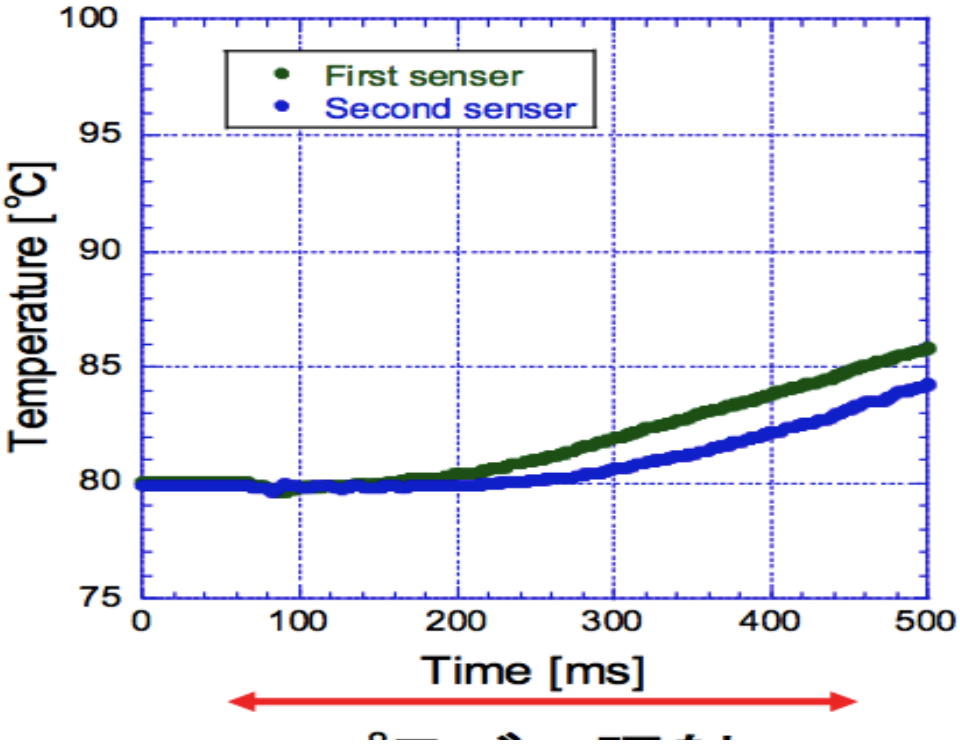

Three thermocouples are embedded. The third TC is connected to support rod (not drawn here) and its time response is very slow.

Comparison of two method

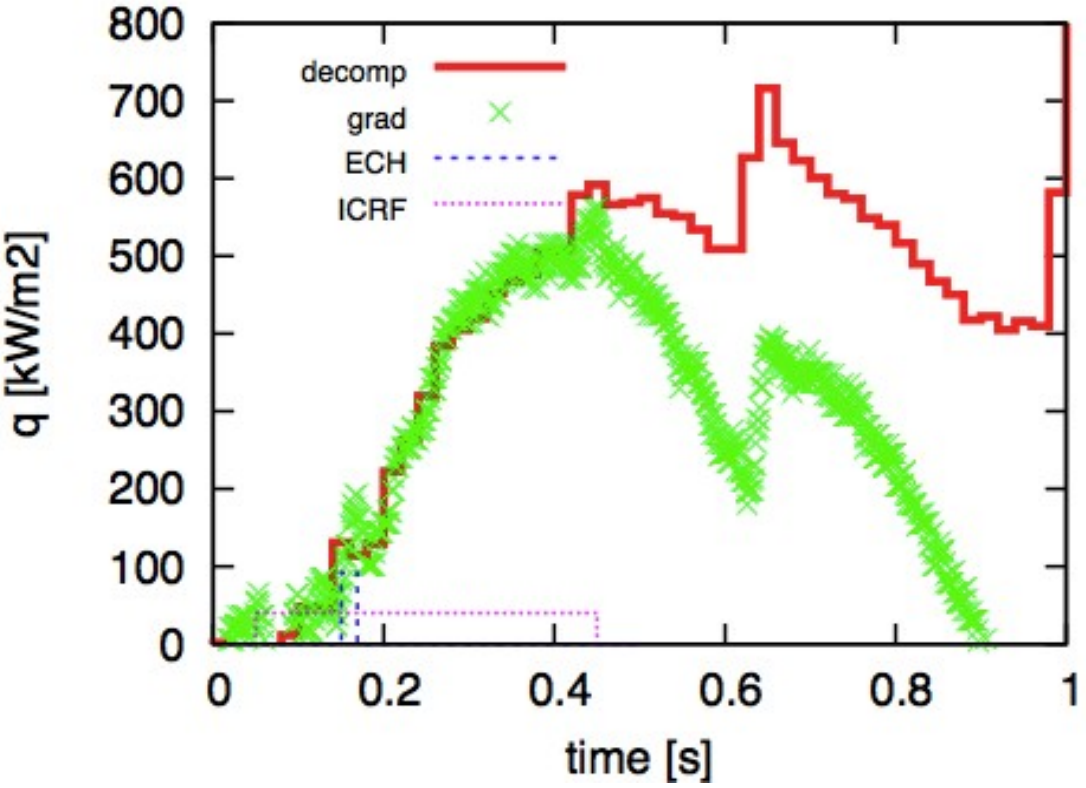

Estimated heat flux with two method agree well *t < 450 ms*.
Pulse decompose method fail to zero value after plasma shot.
This needs further elimination of TC signal noise.

Pulse ECH heating experiment to emulate edge localized mode

EndLoss Ion Energy Analyzer

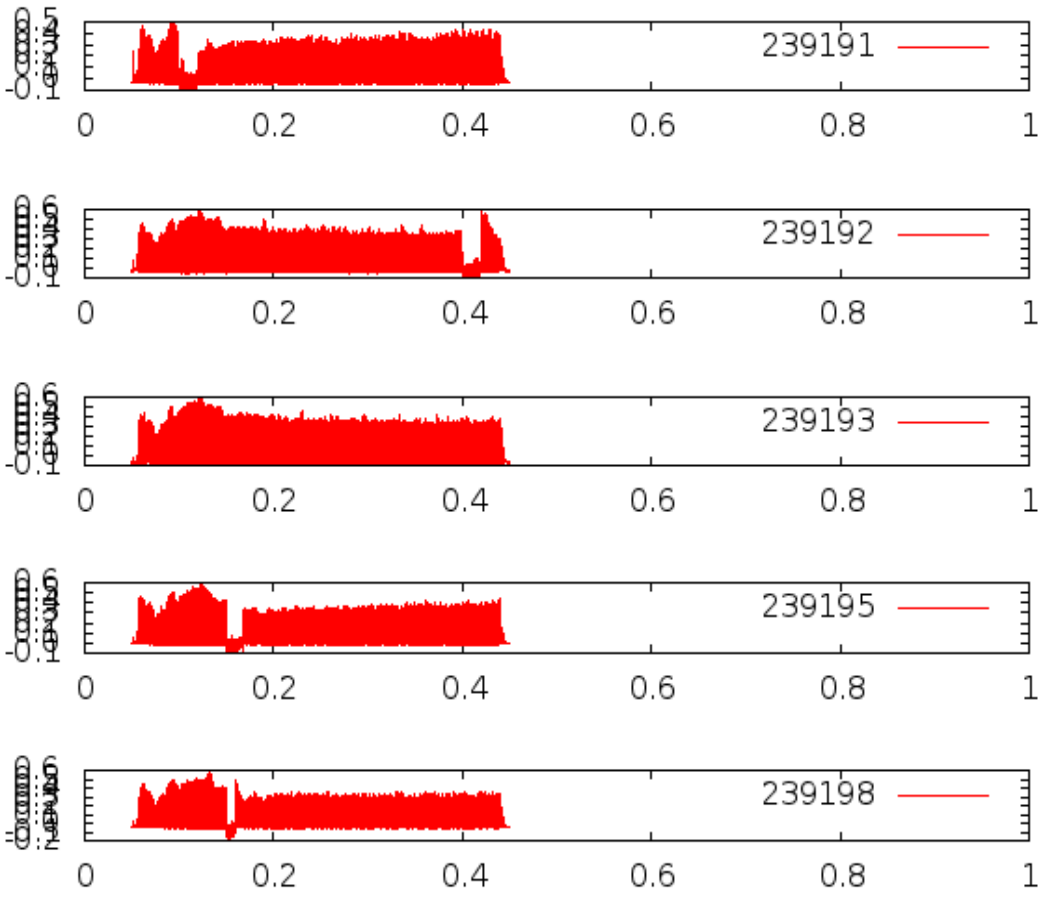

100-120ms, 150kW

400-425ms, 150kW

No pulse

150-169ms, 230kW

150-160ms, 310kW

Results on ELM emulation experiment with ECH pulse

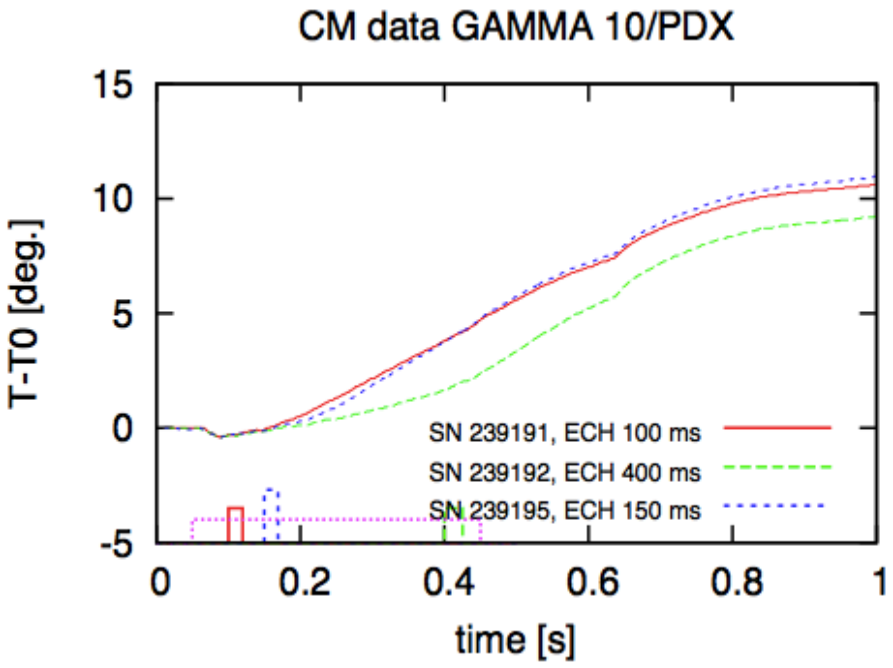

Pulse timing effect with 150 or 230 kW

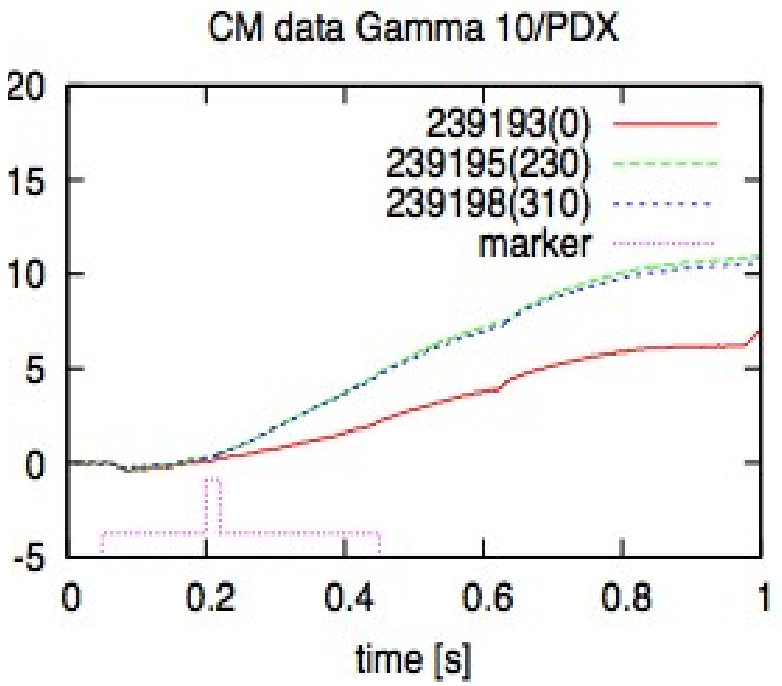

Pulse power effect at 150 ms

Effect of ECH timing

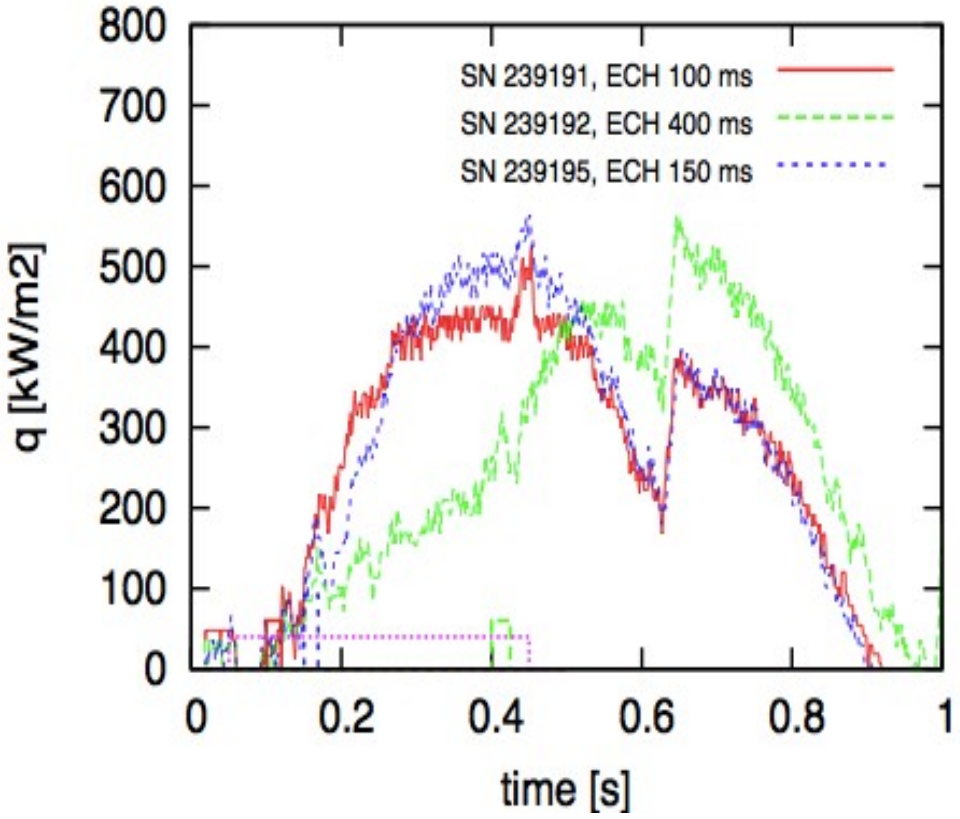

Some time (>50 ms) delay of heat flux exists. (#239192) Its time evolutions are also smoothed out.

Metal sheath of TC junction point might becomes a heat resistance.

Effect of ECH power

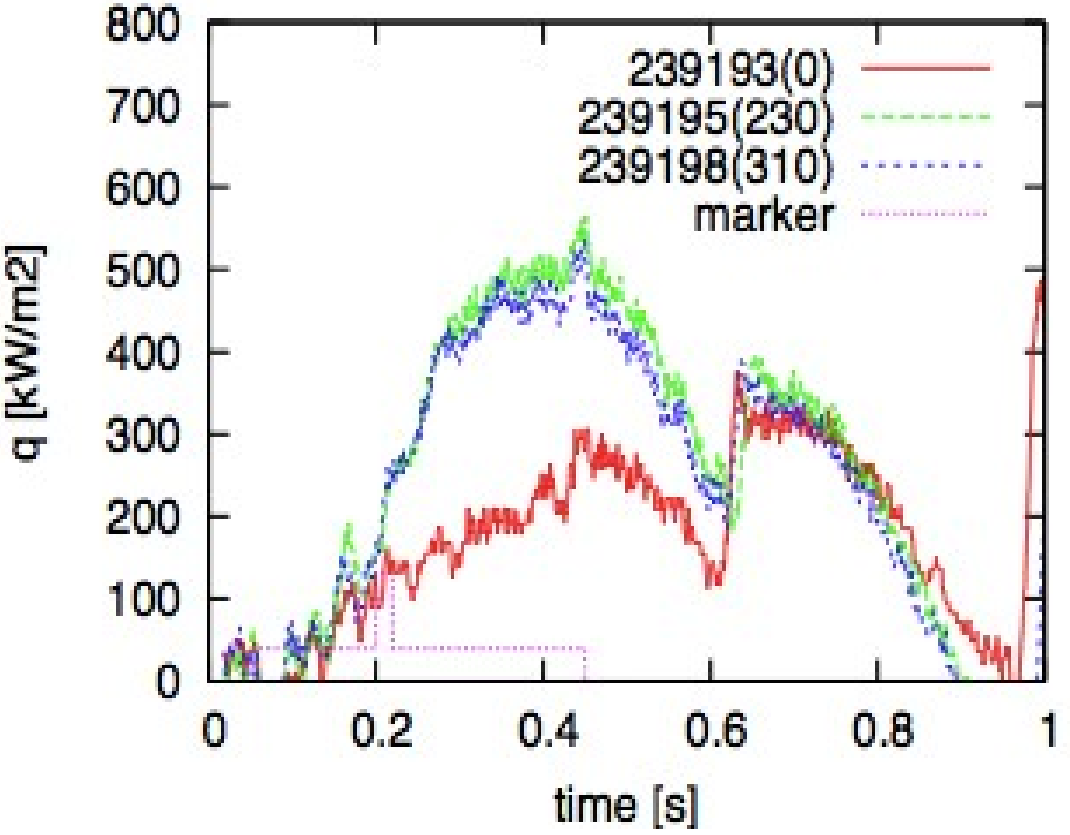

4.6 and 3.1 kJ heating effect for #239195/ 239198. are similar, although they are different from no ECH data.

Japanese PMIF list

(by Prof. Sakamoto)

	APSEDAS	DT-ALPHA	GAMMA10	MAP-II	NAGDIS-II	TPD-Sheet IV
Plasma Source	Inductive/Helicon	Inductive/Helicon	MPD jet / ICRF	PIG, LaB6 DC(80V, < 45A)	LaB6, DC(300V,<200A)	TPD,LaB6 DC(300V,<100A)
Plasma Diameter (m)	0.05	0.04	0.1～0.3	0.05	0.05	0.04 × 0.01
n_e (m^{-3})	< 3 x 10^{18} (D) < 1 x 10^{19} (He)	< 3 x 10^{18} (He)	～10^{19}	< 5 x 10^{17} (H) 2nd < 2 x 10^{18} (He) 2nd < 2 x 10^{19} (He) 1st	< 110^{19} (D) < 110^{20} (He)	~10^{19} (H,He,D)
T_e (eV)	8 - 15 (D) 6 - 11 (He)	2 - 20	~30 only RF ～100 with ECH	1 - 15 (D) 0.05 - 10 (He)	<15 (D) <10 (He)	<10 - 15eV (D,H,He)
T_i (eV)	No Data	No Data	50～400 only RF	0.4-0.6: 2nd 0.035 - 1.0 : 1st	No Data	~ 2eV 2 - 4eV only ICR
Ion Energy (eV)	14 - 50 (D) 14 - 40 (He)	< 2 x 10^4 (He beam)	distributed		< 200	< 100
Flux (m^{-2} s^{-1})	< 5 x 10^{22} (D) < 10^{23} (He)	< 10^{22} (plasma) < 10^{20} (beam)	< 10^{23} (10^{24})	10^{22}-10^{23}	< 5 x 10^{22} (D) < 10^{23} (He)	<10^{23}
Plasma Duration	Steady state	Steady state (design) 1-10 s (typical)	< 0.4 s (10s)	Steady state	steady state	Steady state
Neutral Pressure (Pa)	~2.7 (D) ~4.7 (He)	0.3 - 30	No Data	0.2-20	~ 0.1-1	~ 0.1-2
B (T)	< 0.05 T	< 0.2	0.15～1.5	< 0.03 T	<0.25 T	<0.12T
Target Material	W, Mo, metals	(SUS)	W, C, etc.	W, C, Mo (Thermal Probe)	W, Mo, C, SUS	W, Mo, metals
Others			Heat flux (MW m^{-2}): 1.0 only RF < 9.0 with ECH	Degree of dissociation: 0.8-5% Mach Number //: 0.1-0.2 Neutral Tem.: 0.04-0.07 eV Negative ion density H^-: 10^{14}-10^{16} m^{-3}		Negative ion density H^- D^-: <10^{15} m^{-3}

Divertor simulator TPDSheet-IV

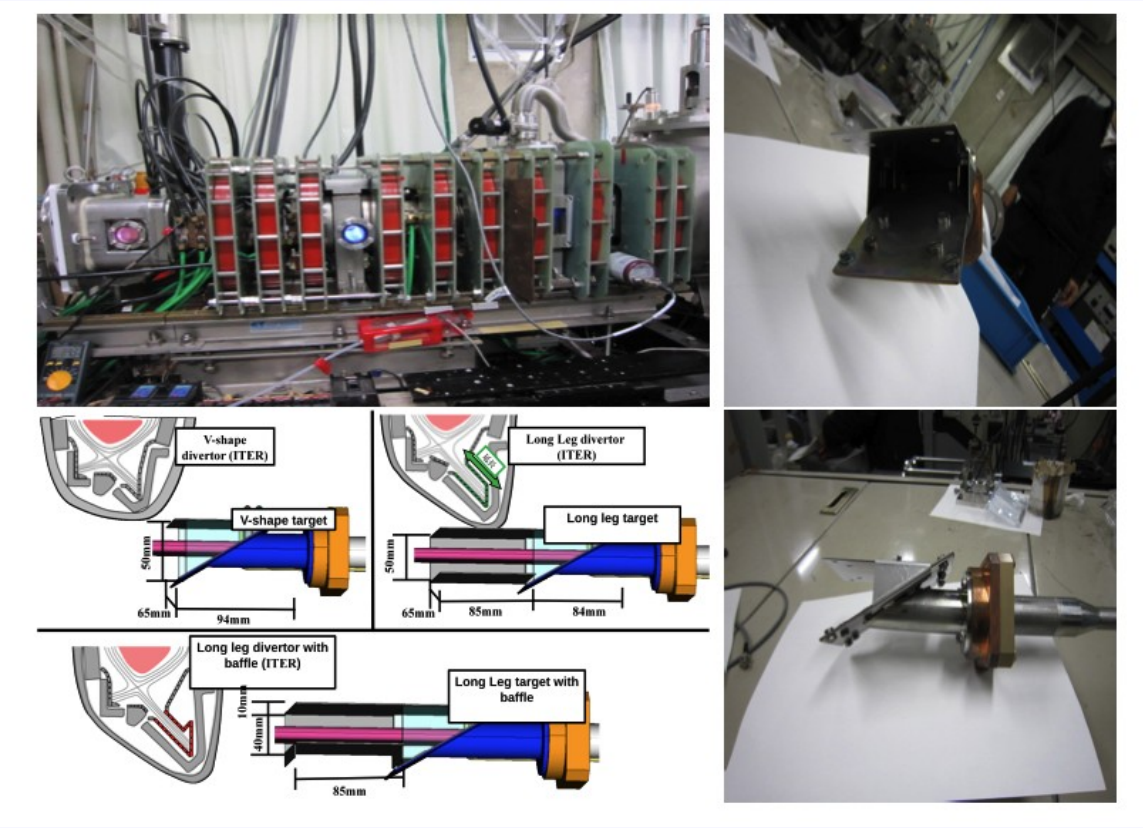

Laboratory size linear plasma device in Tonegawa Laboratory, Univ. Tokai.

DEGAS 2

DEGAS 2 neutral transport simulation code is the successor to old DEGAS code, and has a new mesh generator utility, which makes it easier to modify target geometry and to compare its effect on neutrals.

By using DEGAS 2,

- Dynamic memory allocation is possible. (Fast and large scale simulation for cheap PC) • 2D Certician model geometry (like TPD–SheetIV) can be constructed.
- Future expansion of simulation seems easier with the help of PPPL author.

Current limitations or problems are

- Neutral source assignment is still an open question. So absolute value of neutral density needs other calibration with experimental data.
- To calculate H alpha line-integrated intensity and spectra shape is not examined, since detectors information and larger number testflight are needed.
- Some atomic process data in detached plasma might be lacking. (In PSI21, we tried to improve this situation.)

What we did with DEGAS 2

Mesh geometries to check effect of target angle, closed target, duct length, gas puff position, etc.

Plasma profile change by detachment

Collisional radiation model to deal molecular ion by Hollmann, which makes important roll in molecular assisted recombination process

Mesh model production

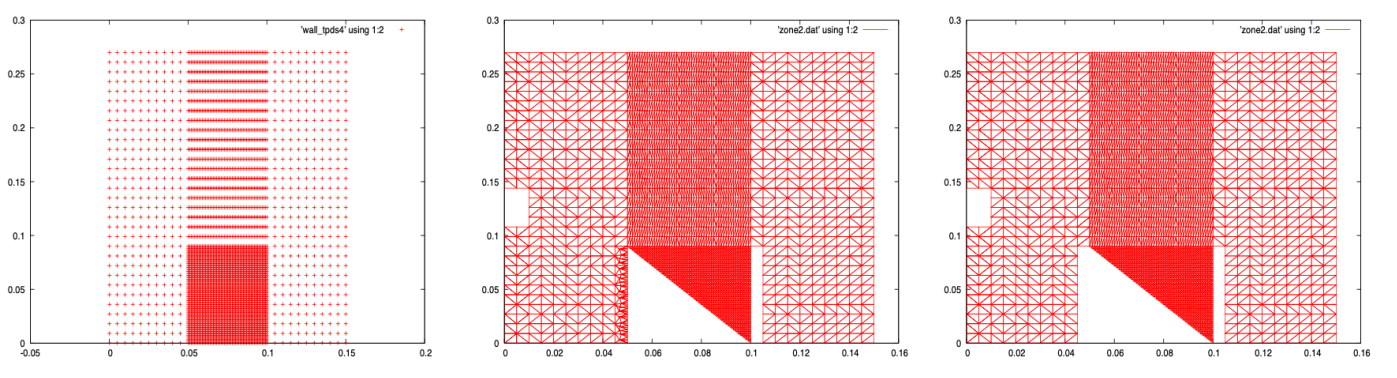

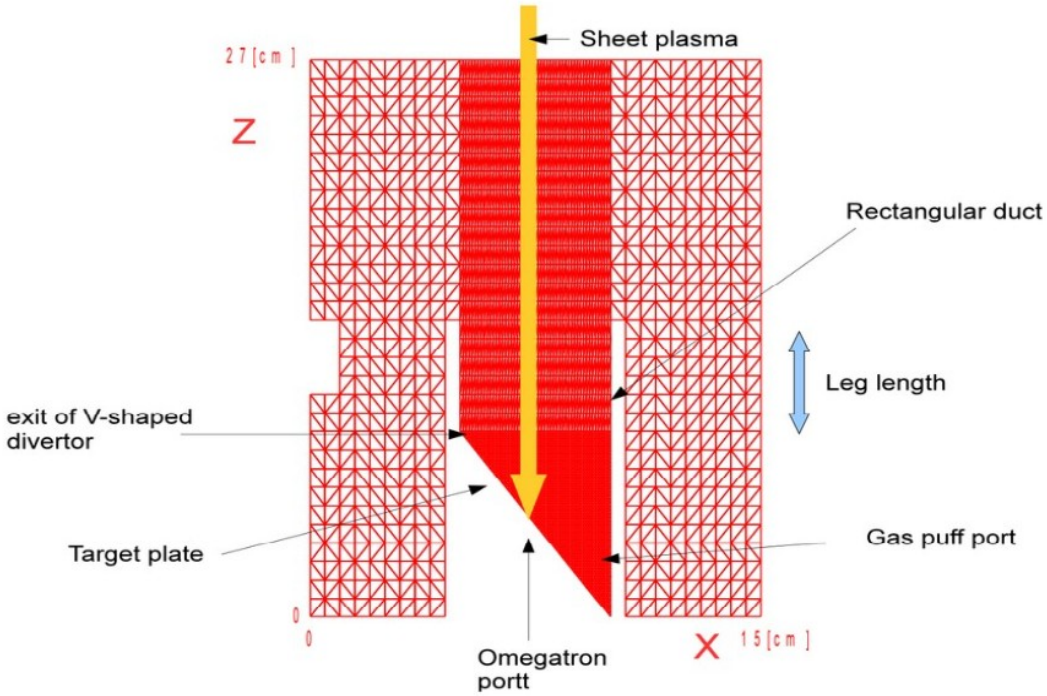

Fig. 1 Schematic view of the model geometry of TPD-SheetIV experimental region. Divertor leg plasma is simulated by the sheet plasma of this device. So the foot-point is the divertor plate surface where the sheet plasma hits. Leg length is correspond to that of the rectangular duct connected to the exit of the V-shaped divertor. In this figure, leg length is 81 mm. Gas puff port is set near the corner of the V-shaped divertor.

Detached plasma profile

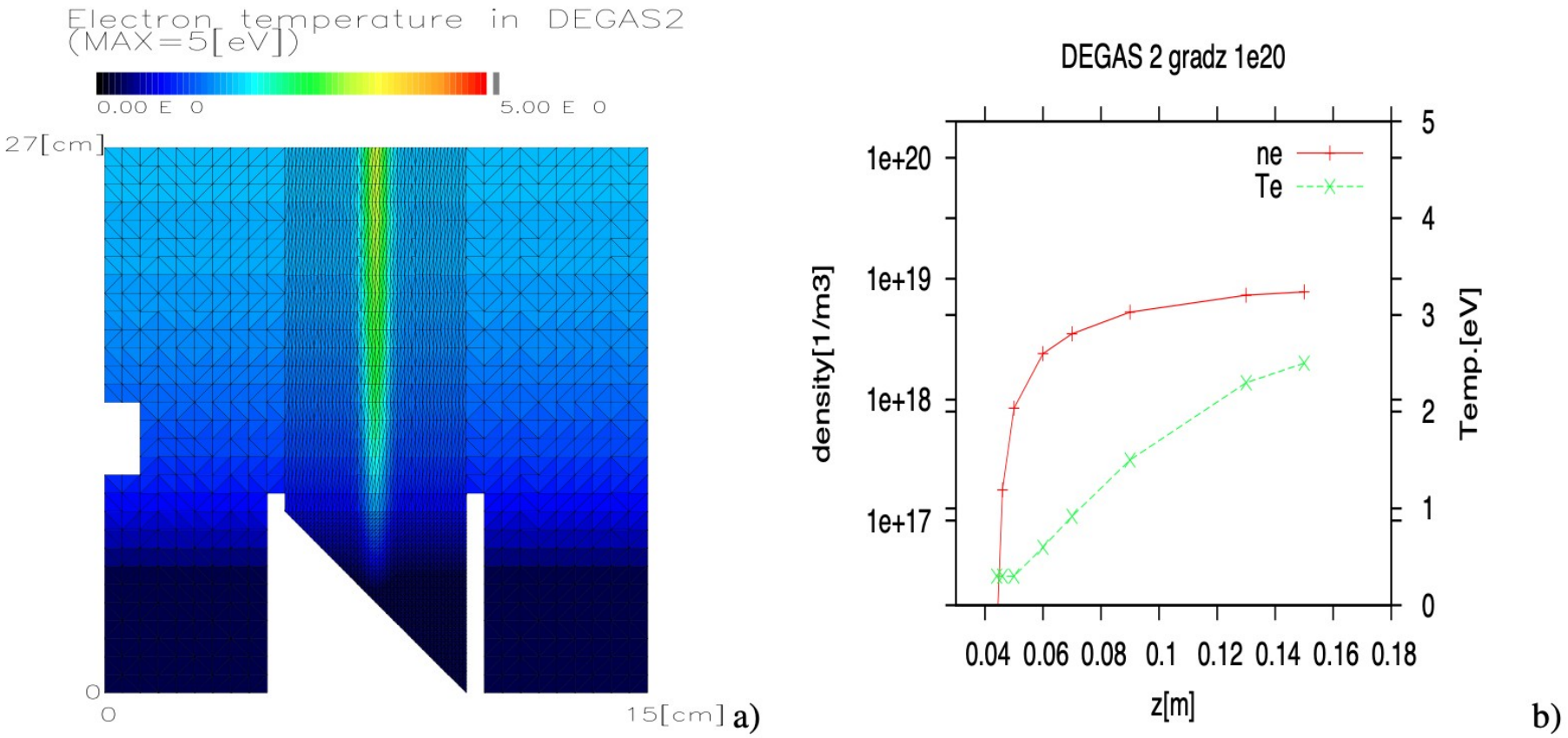

Fig. 2 Electron temperature profile assumed in DEGAS 2 simulation (a),2-dimensional, b) 1-dimensional along sheet plasma). $a_1(x)$ in eq(1) is a gauss function, and $a_3 = 50$ mm and $a_4 = 0.3$ eV are used in this figure.

Molecular ion production and destruction reactions

Target	acronym	Reaction expression	
H	eI	$e + H \rightarrow 2e + H^+$	
H_2	DA	$H_2 + e \rightarrow H^- + H$	not used
	eD	$H_2 + e \rightarrow H + H + e$	
	CNV	$H_2 + H^+ \rightarrow H_2^+ + H$	
	BCNV	$H_2^+ + H \rightarrow H_2 + H^+$	
	eI2	$H_2 + e \rightarrow H_2^+ + e + e$	
	eDI	$H_2 + e \rightarrow H^+ + H + e + e$	
	eDn	$H_2 + e \rightarrow H^* + H + e$	
H_2^+	DR2	$H_2^+ + e \rightarrow H^* + H$	
	eD2	$H_2^+ + e \rightarrow H^+ + H + e$	
	eDI2	$H_2^+ + e \rightarrow H^+ + H^+ + e + e$	
	CNV2	$H_2^+ + H_2 \rightarrow H_3^+ + H$	
H_3^+	DR3	$H_3^+ + e \rightarrow H_2^+ + H + e$	
	DR3	$H_3^+ + e \rightarrow H + H + H$	
	BCNV2	$H_3^+ + H \rightarrow H_2^+ + H_2$	

Table 1: Related reactions. Acronyms for each reactions are the same as those in Hollman et al., Phys. Plasmas 9 (2002) 4330-4339.

Ion balance equations

In steady state, ion densitys (N_1 for H^+, N_2 for H_2^+, N_3 for H_3^+) obey the following equations, where S is rate coefficient for each reaction and given as the function of electron temperature and vibration temperature of hydrogen molecule.

$$\begin{aligned}\frac{dN_1}{dt} = 0 \quad = \quad & N_H N_e S_{eI} - N_{H_2} N_1 S_{CNV} + N_2 N_H S_{BCNV} \\ & + N_{H_2} N_e S_{eDI} + N_2 N_e S_{eD2} + 2 N_2 N_e S_{eDI2}\end{aligned} \tag{1}$$

$$\begin{aligned}\frac{dN_2}{dt} = 0 \quad = \quad & N_{H_2} N_1 S_{CNV} - N_2 N_H S_{BCNV} + N_{H_2} N_e S_{eI2} \\ & - N_2 N_e S_{DR2} - N_2 N_e S_{eD2} - N_2 N_e S_{eDI2} \\ & - N_2 N_{H_2} S_{CNV2} + N_3 N_e S_{eD3} + N_3 N_H S_{BCNV2}\end{aligned} \tag{2}$$

$$\frac{dN_3}{dt} = 0 = N_H N_2 S_{CNV2} - N_3 N_e S_{eD3} - N_3 N_e S_{eDR3} - N_3 N_H S_{BCNV2} \tag{3}$$

If the data of DEGAS 2 simulation data for neutral density (N_H and N_{H_2}) is used, these equation is simultinouse linear equation ($A\vec{x} = \vec{b}$) and easily solved with Gauss's elumination method, where A is the matrix defined as

$$A = \begin{bmatrix} N_{H_2} S_{CNV} & -N_H S_{BCNV} - N_e S_{eD2} & 0 \\ & -2 N_e S_{eDI2} & \\ -N_{H_2} S_{CNV} & N_H S_{BCNV} + N_e S_{DR2} & -N_e S_{eD3} - N_H S_{BCNV2} \\ & + N_e S_{eD2} + N_e S_{eDI2} & \\ & + N_{H_2} S_{CNV2} & \\ 0 & -N_H S_{CNV2} & N_e S_{eD3} + N_e S_{eDR3} \\ & & + N_H S_{BCNV2} \end{bmatrix} \tag{4}$$

and $\vec{x} = (N_1, N_2, N_3)$

$$\vec{b} = (N_H N_e S_{eI} + N_{H_2} N_e S_{eDI}, N_{H_2} N_e S_{eDI2}, 0) \tag{5}$$

Effect of duct length

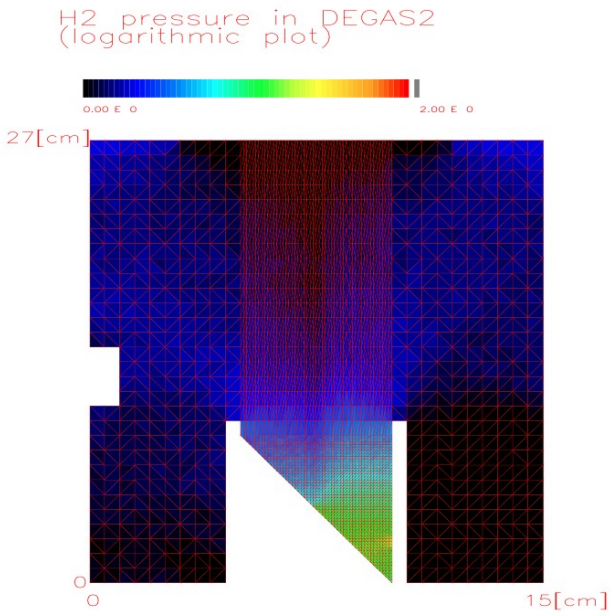

9

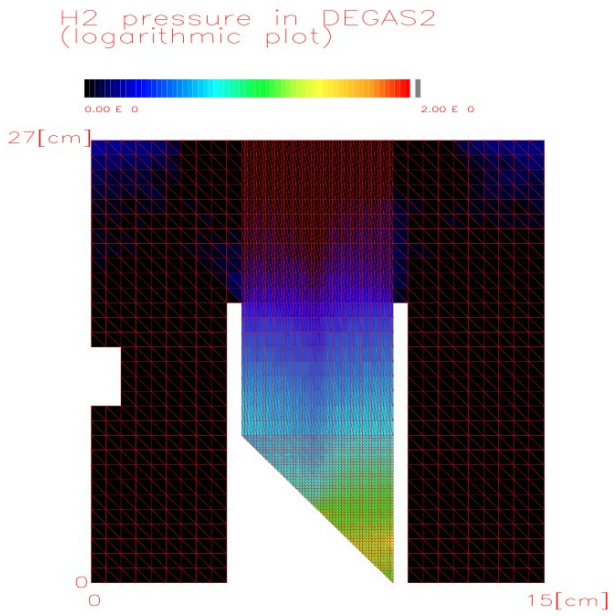

81

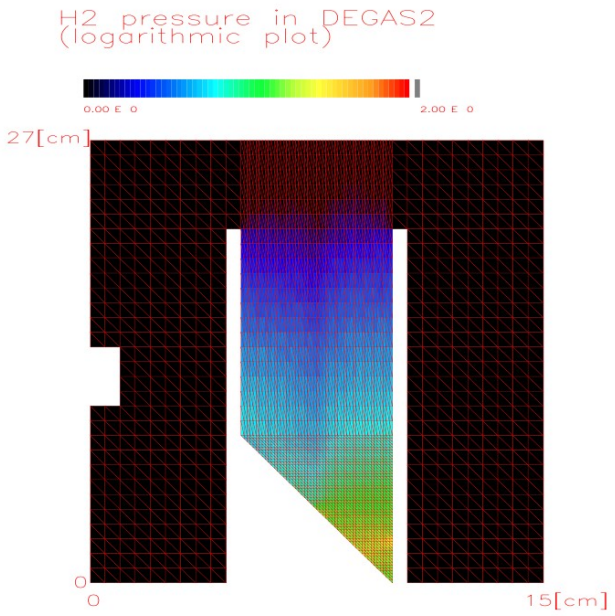

126[mm]

These results show that long2-leg target (leg14, 126mm) can induce MAR reaction effectively because of increasing H2 pressure.

Results for long leg divertor

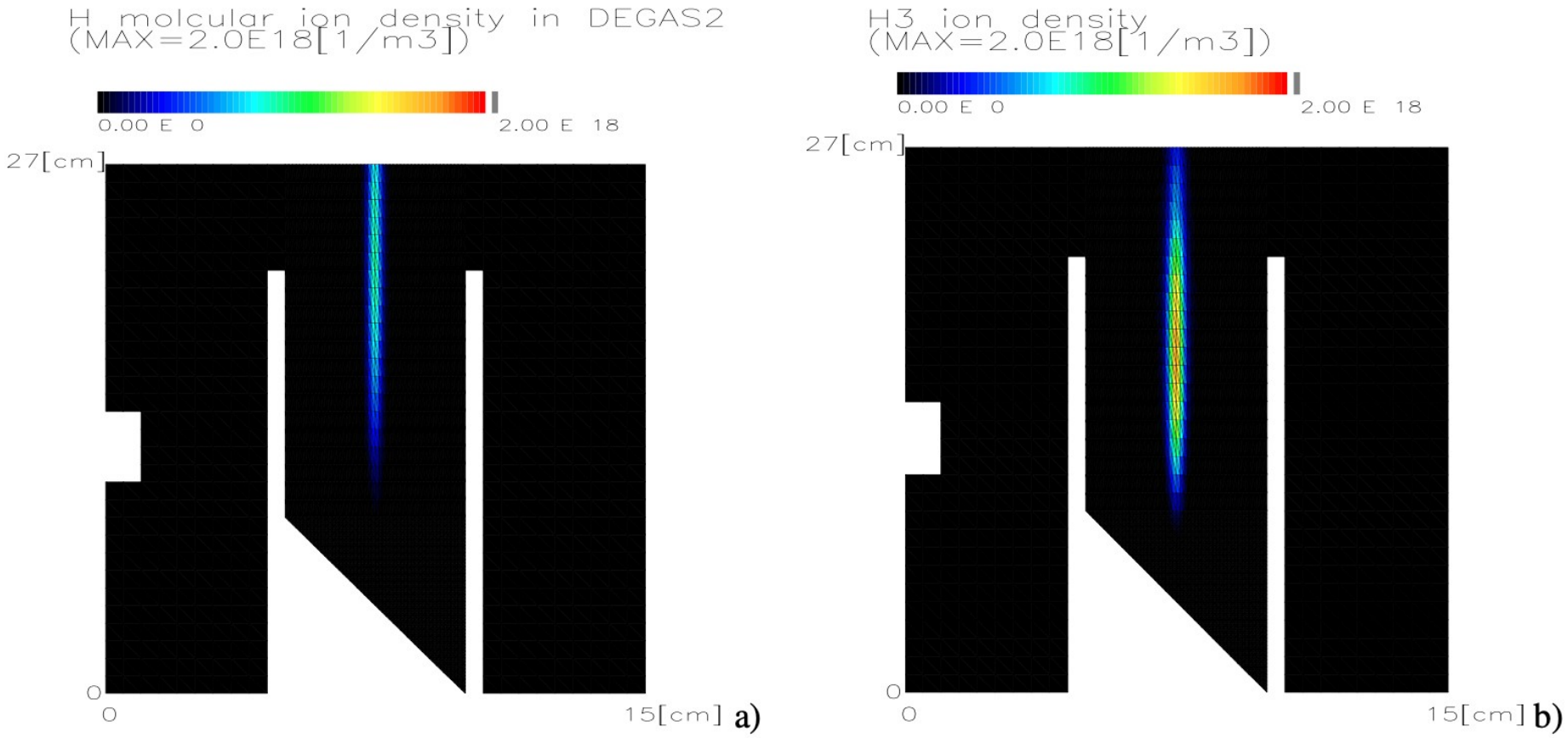

Fig. 5 Comparison of molecular ion profile for long leg divertor configuration. a) is H_2^+ and b) is H_3^+.

Conclusion

- Reliable estimation method of heat flux onto plasma facing materials is an important tool to solve thermal problem in nuclear fusion technology.

- To do it, time dependent heat balance in CVs must be treated carefully.

- Two analysis methods (gradient method and pulse decompose method) were successfully applied for various fusion plasma experiments.(GAMMA 10/PDX, LHD)

- Now heat flux onto divertor tile in demo reactor is the next research target.

Conclusion(2)

- Neutral behavior in TPDSheet–IV is studied with DEGAS 2 and its definegeometry2d and defineback module.
- Hydrogen molecular ion production process is modeled with Hollman's data, and its calculation is applied to zone by zone DEGAS 2 results.
- In detached region, neutral density is large, but H-alpha intensity decreases since electron density is small.
- The long-leg divertor is expected to induce MAR due to increasing H2 as compared to V-shaped target.

Thank you for kind attention

Cảm ơn bạn đã quan tâm

ご清聴ありがとうございます

Appendix

Plasma parameters

	Atmospheric plasma	Fusion plasma
size	0.1~10 mm	1~10 m
Neutral gas press.	＞1atm =10^5 Pa	< 1 Pa
Electron density	10^{11} ~ 10^{15} cm^{-3}	10^{12} ~ 10^{15} cm^{-3}
Temperature	Te(>>Ti) = 1~10 eV	Te (~ Ti) = 0.1 ~ 10 keV
Heat flux	< 1 kW/m^2 (earth surf.)	~10 MW/m^2 (sun surf.)
Reaction	Chemical reaction	Nuclear reaction

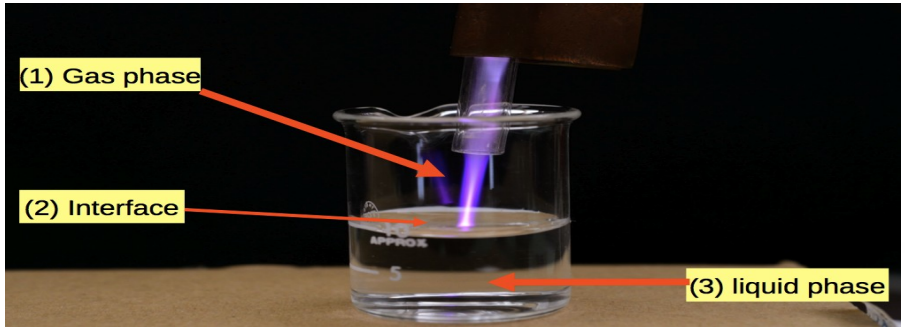

Divertor thermal design study

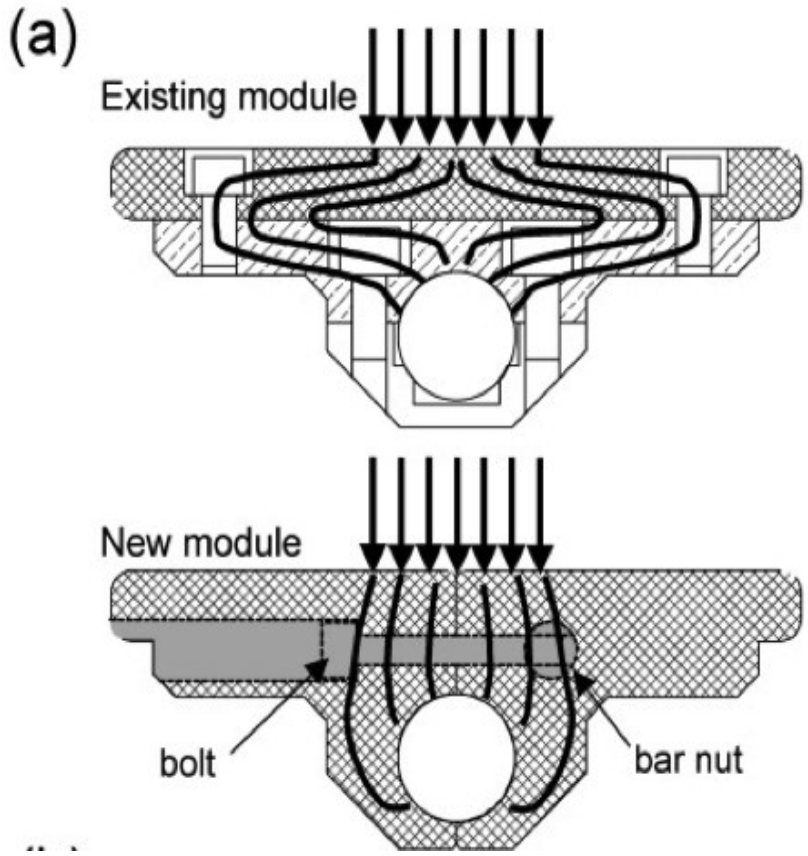

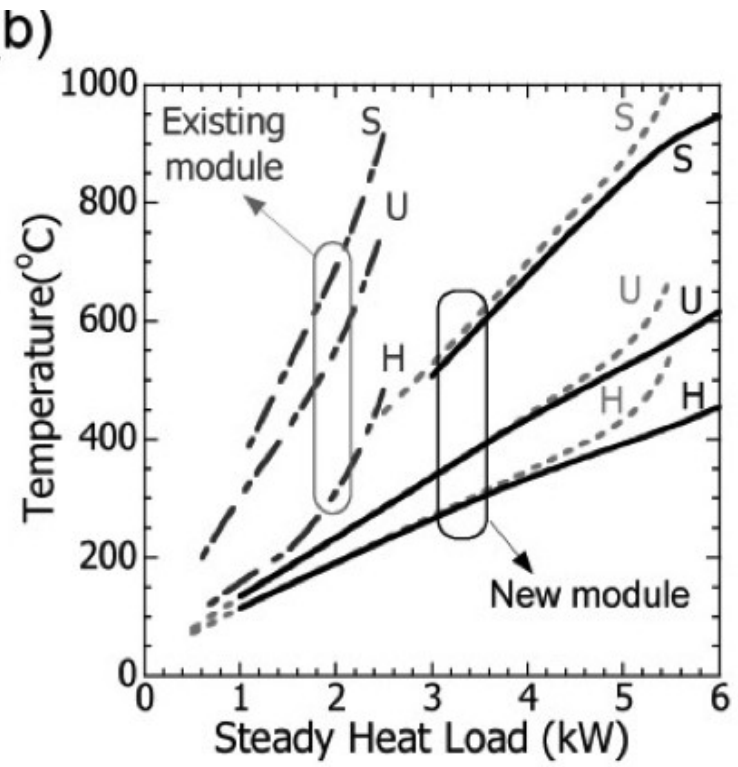

Diveror structure and materials are optimized to reduce surface temperature below the melting point.

Masuzaki:
FST Vol.50(2006)361

Effect of radiation defect in divertor structure material

- Heat conductivity (thermal diffusivity) is the most important parameter to design divertor cooling.

- Its basic mechanism is phonon conductivity for ceramic (SiC), and phonon-lattice scattering is increased with defect induced by neutrons.

- This phonon transport is also important for tungsten (W).

Degradation of Thermal Conductivity in Ceramics

Divertor of Fusion Reactor

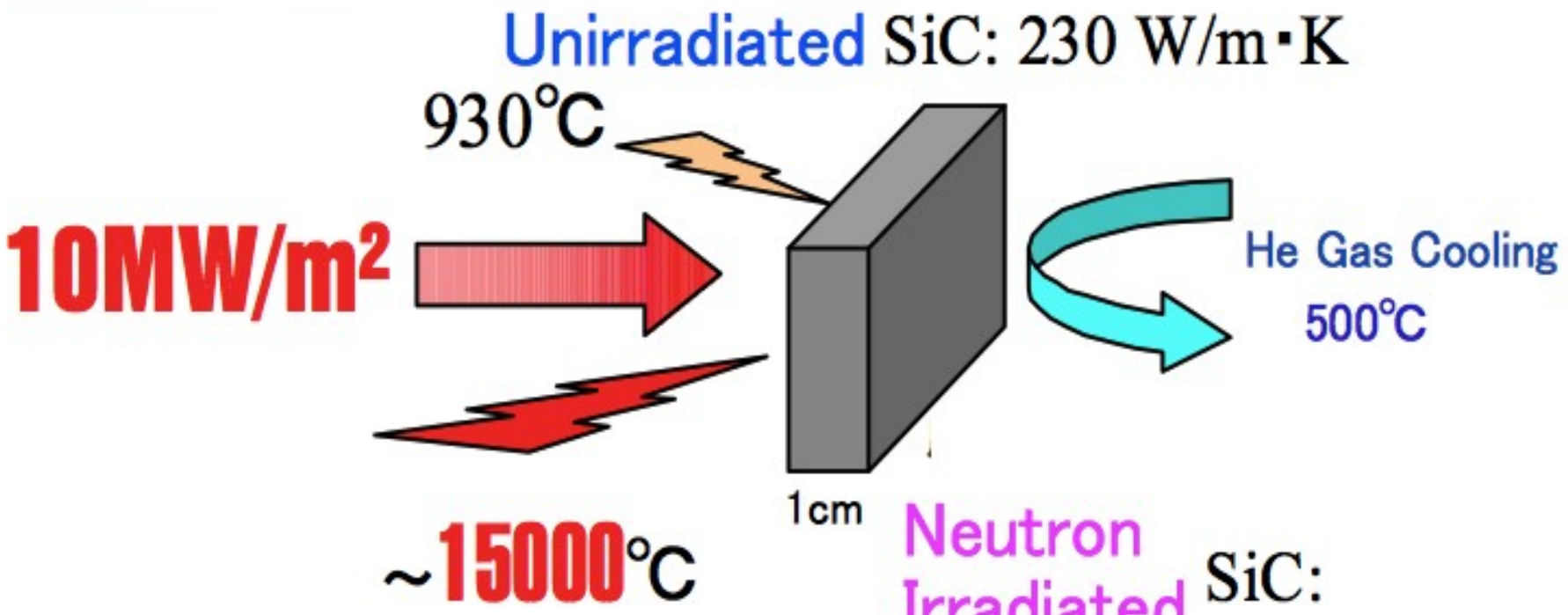

Ceramic thermal property is drastically reduced under neutron irradiation.

Thermal Diffusivity of Ceramics

- Heat is mainly carried by phonon unlike metals.
- In non-irradiated materials, thermal diffusivity is affected by microstructure of grain that was changed with sintering process.

Thermal Diffusivity $\alpha = 1/3 \cdot \mu \cdot \lambda$

μ : Mean speed of phonon [m/s]

λ : Mean free path of phonon [m]

In an irradiated specimen, mean free path of phonon is decreased to very small and the grain structure is too large to affect to the thermal diffusivity.

$$1/\lambda = 1/\lambda_a + 1/\lambda_b + 1/\lambda_c \cdots$$

Almost constant with each material

Phonon-Phonon Scattering

Changes with the temperature T as k/T^n (for non-irradiated single crystal, n=1)

Phonon-Lattice Scattering

Increased with density of irradiation defects

Temperature change must be compensated before estimation.

Irradiation dose rate affects defect formation rate.

Temperature Change

After the Irradiation

During the Irradiation

Estimation of Thermal Diffusivity During the Irradiation

Post irradiation measurement at the irradiation temperature represent the thermal diffusivity during the irradiation.

3 Assumption

1. Post irradiated specimens kept the same amount of defects as during the irradiation
2. Defects were stable until annealed above the irradiation temperature
3. Degradation of thermal diffusivity with neutron dose was saturated ~ 3×10^{26}n/m^2

Thermal diffusivity at the irradiation temperature

$\alpha_{irr}=k/T_{irr}^{n}$

T_{irr}: the Irradiation Temperature

k, n: fitting parameters obtained from measurement of thermal diffusivity with various temperature

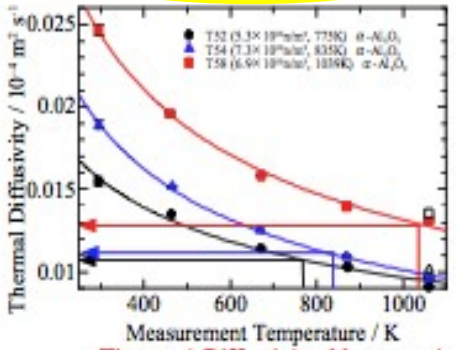

Thermal Diffusivity Measured at Elevated Temperature

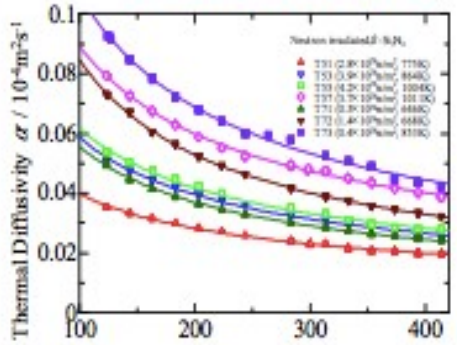

Thermal Diffusivity Measured below the irradiation temperature

Problem

Test Irradiation	Irradiation temperature was controlled to the objective temperature
Real Divertor	Temperature of a material will be changed with injected heat flux and density of defects

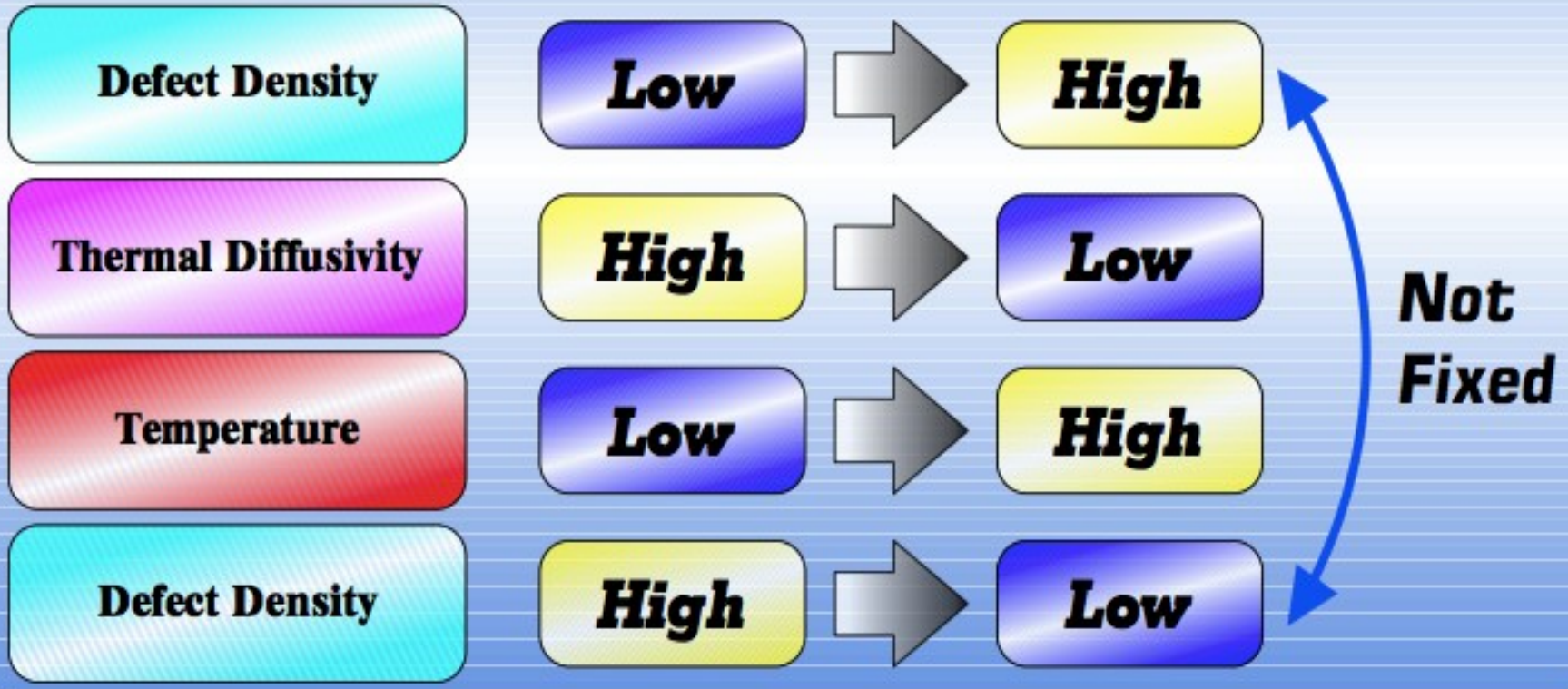

Analysis based on Reaction Kinetics is required

Inverse problem of heat conduction

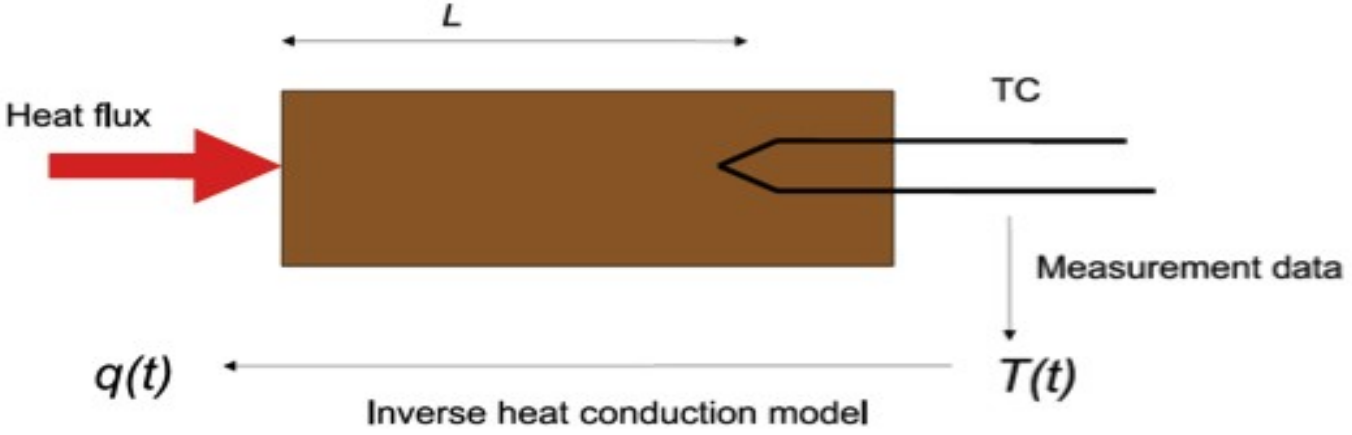

(a) Long pulse plasma

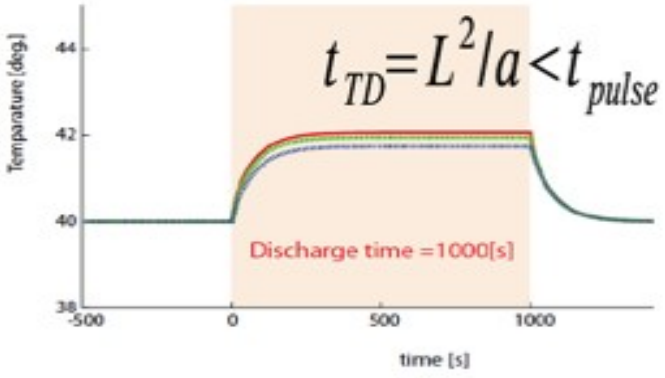

(b)Short pulse plasma

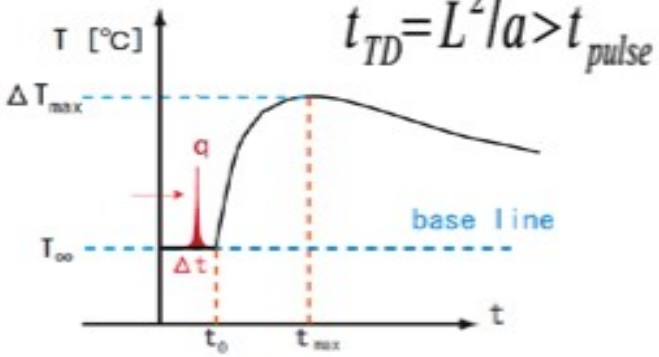

ダイバーター模擬装置
MAP-II, TPD-SheetIV

中型核融合実験装置
Heliotron J, Gamma 10

Lumped-Heat-Capacity system approximation

The smaller size of CV, the more accurate heat balance.
For small CV, if characteristic time of head load evolution is smaller than thermal diffusion time, temperature profile in CV could be neglected in heat balance.

This corresponds to mass of center approximation in rigid body motion.

Insulated (h=0) calorimeter satisfy this small Biot number(hV/kS~hL/k) condition easily.

Boundary condition of backside

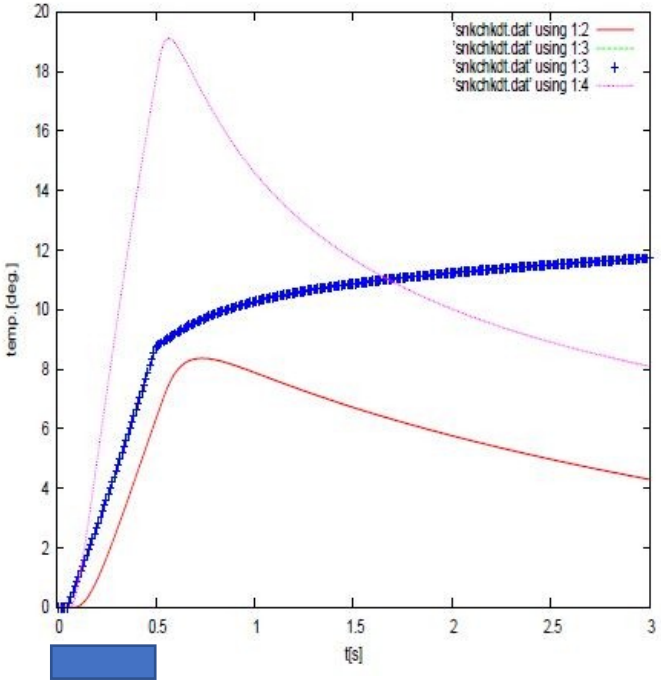

According to boundary condition, temperature evolution for same heat flux injection will be different.

So heat flux estimation with proper boundary condition can only give reasonable value from measured temperature data.

Heat

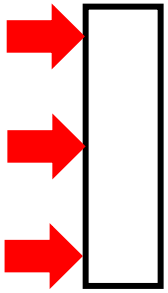

Insulation (Blue)

Qout = 0

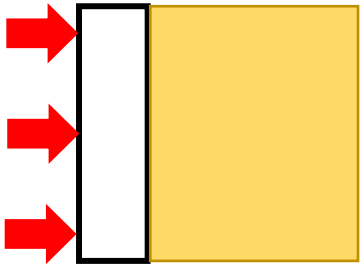

...

Infinity(Magenta)

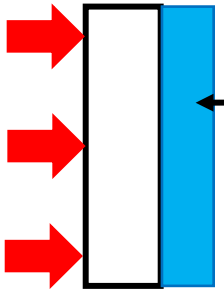

Ideal heatsink
(Nothing increase of temperature)

Qout = ∞

Sink(Red)

Thermal insulation boundary model

Even when the shape of a object (or CV) is complicated, if heat outflux or heatloss through boundary can be neglected compared with heat influx, it could be assumed to be isothermal and heat balance can be estimated by very simple equation.

$$qS = c\rho V \frac{dT}{dt} \sim c\rho V \frac{\Delta T}{\Delta t}$$

Insulated calorimeter temperature evolution is a linear function of time for constant heat flux.

Thin film temperature response

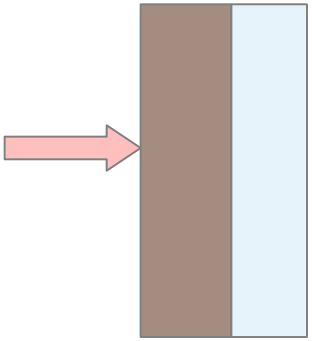

```
# t_0[s], temp_0[deg.C], t_pulse[s], q_inf[W/m2]
  0.050d0, 0.0d0, 0.450d0, 0.5d6
# al1[m], al2[m], al_end[m], eta_t
  0.0012d0, 0.0008d0, 0.002d0, 0.0
# x_st[m], x_end[m], x_step[m], x_1, x_2, x_3
  0.0d0,  0.0018d0, 2.0d-5, 0.0002d0, 0.0010d0, 0.0018d0
```

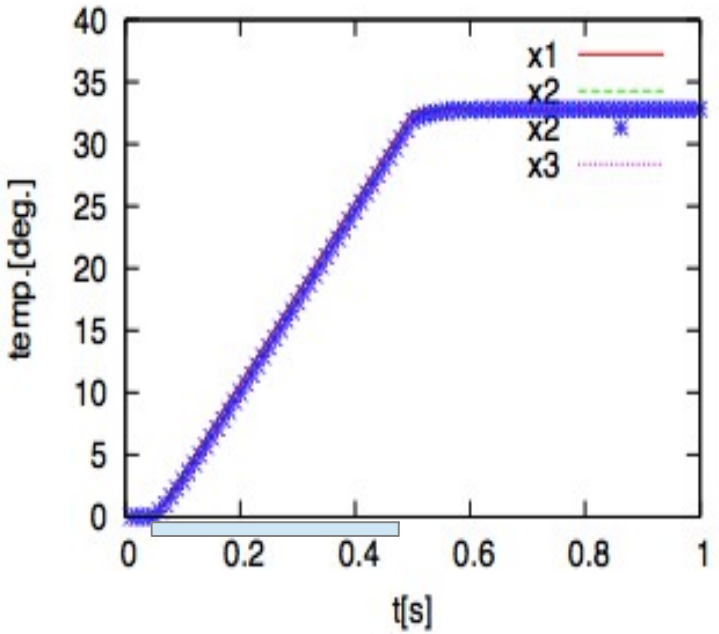

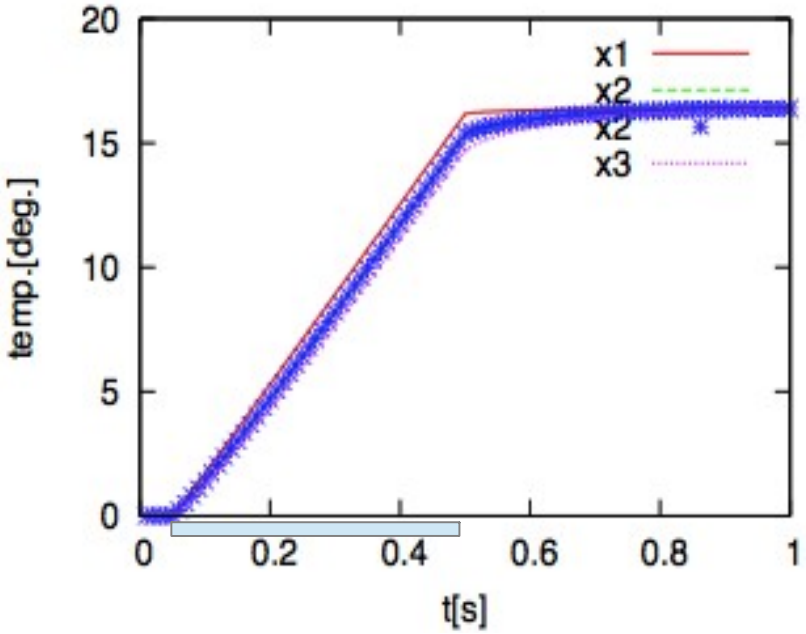

Emulate small heat loss with thickness of 4mm

Effect of boundary condition at backside surface

```
# input parameter for snkchk.exe
# t_0[s], temp_0[deg.C], t_pulse[s], q_inf[W/m2]
  0.050d0, 0.0d0, 0.450d0, 0.5d6
# t_st[s], t_end[s], t_step[s], t_1, t_2, t_3
  0.0d0, 5.0d0, 1.0d-2, 0.35d0, 0.55d0, 1.0
# al1[m], al2[m], al_end[m], eta_t
  0.0012d0, 0.0008d0, 0.000d0, 0.0
# x_st[m], x_end[m], x_step[m], x_1, x_2,
  0.0d0   0.0018d0  2.0d-5  0.0002d0, 0.00
```

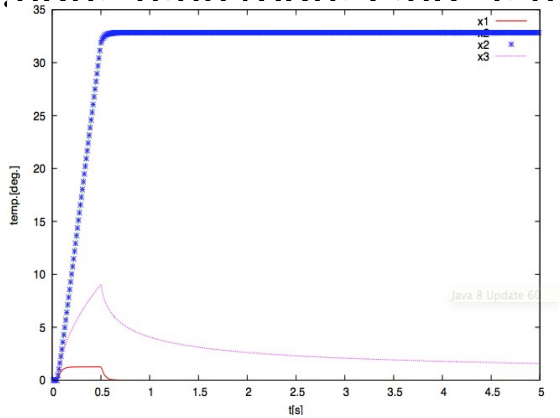

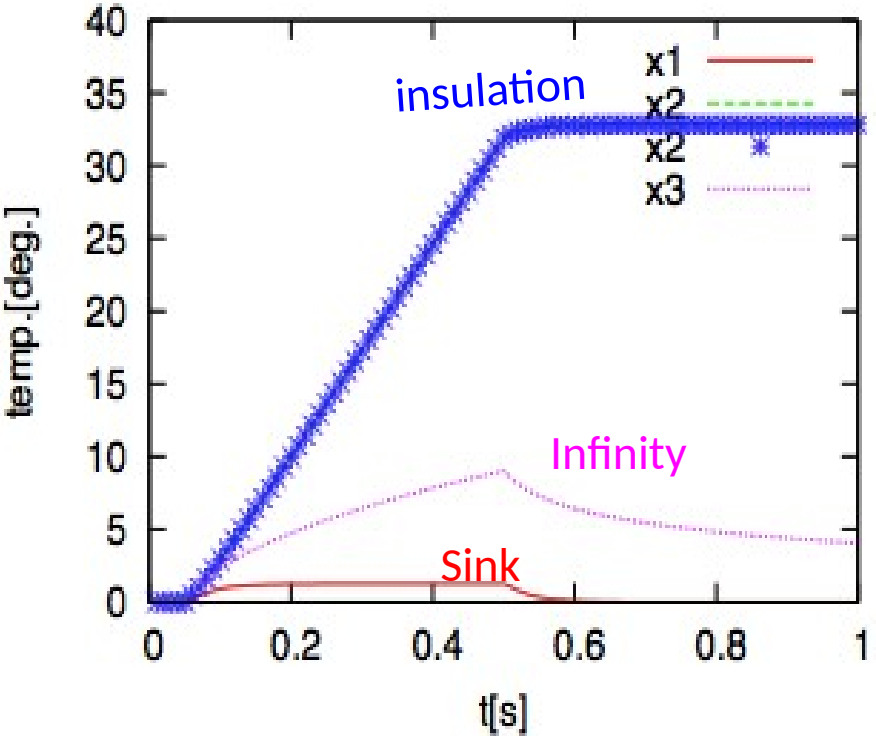

Insulated calorimeter has good SN ratio.

Heat flux in PM-CuspDEC

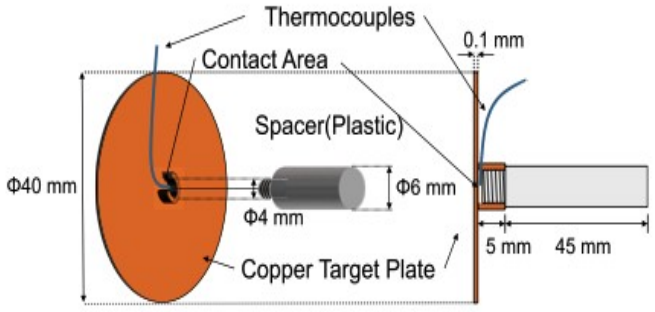

Fig. 3 Schematic image of the calorimeter.

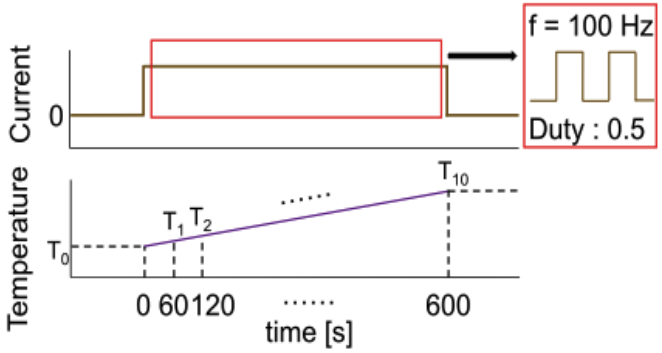

Fig. 6 The schematic image of time evolution of the inflow current and the temperature depending on the exposure time.

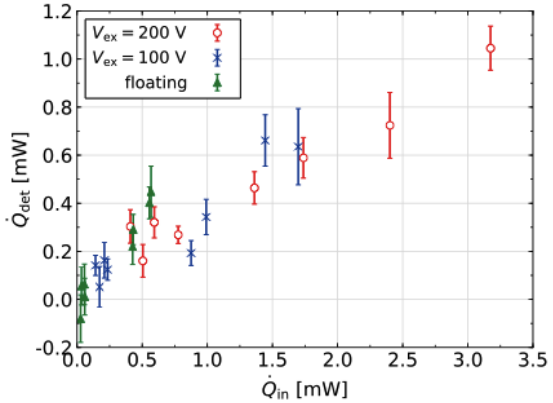

Fig. 7 The detected rate of heat flow vs. the incident rate of heat flow.

Nonda and Takeno
PFRVolume 13, 3405050 (2018)

Very small heat flux was estimated with insulation boundary model.

Heat flux estimation in CuspDEC

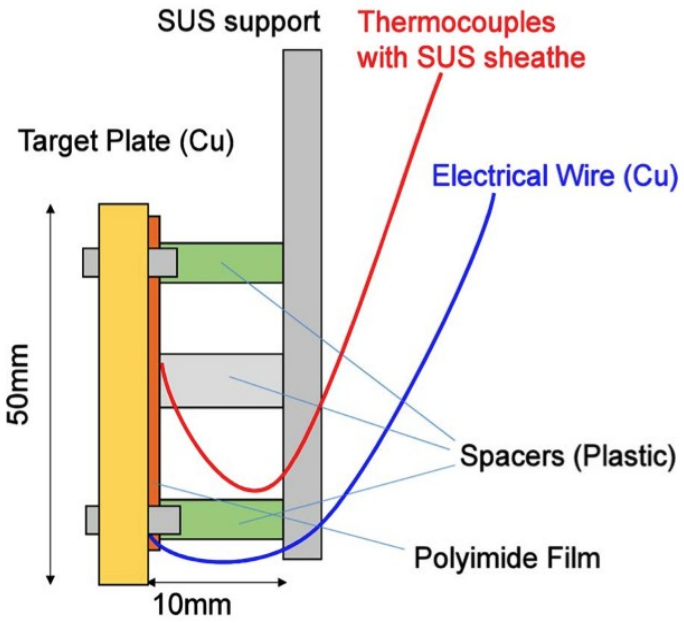

Fig. 4. Schematic design of the calorimeter.

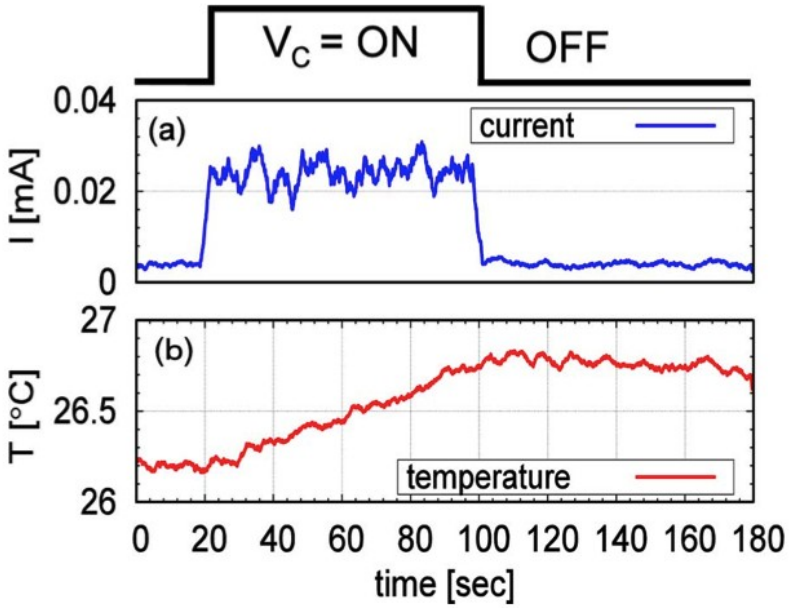

Fig. 3. Typical time evolution of (a): target current and (b): target temperature during beam exposure.

Temperature peak appears just at pulse end.

Ichimura et al,: Fusion Engineering and Design
https://doi.org/10.1016/j.fusengdes.2018.02.046

Fitting to TC data

Some contribution can be negative.

A pair of positive and negative ones with same amplitude consist a pulse.

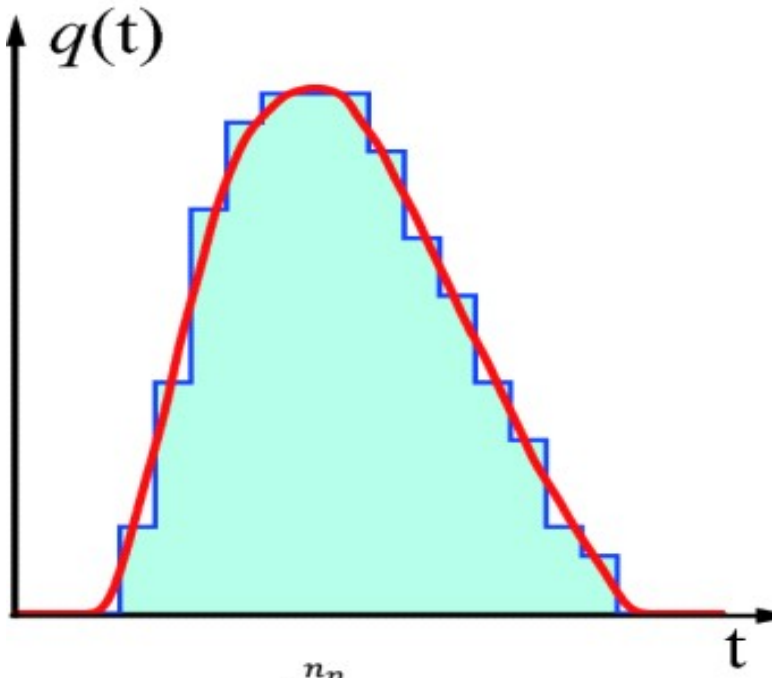

$$q(t) \sim \sum_{i=1}^{n_p} q_0 C_i H(t - t_i)$$

The size of each step C_i is determined so as that the summation of their temperature response reproduces the observed temperature variation data.

$$T(t) - T_0 \sim \sum_{i=1}^{n_p} C_i S_i(t) \qquad (2)$$

Fitting with iterative least square method

The square of residue between TC data and known approximate function

$$D_i = \sum_j (C_i S_i(t_j) + F_{i-1}(t_j) - T_j)^2$$

$$F_i(t) = \begin{cases} 0 & (i = 1) \\ \sum_{k=1}^{i} C_k S_k(t) & (i = 2, \ldots, n_p) \end{cases} .$$

is minimized only with 2*MTP data around t=tj個, and hence, Ci is determined as following.

$$C_i = \sum_j S_i(t_j)(T_j - F_{i-1}(t_j)) / \sum_j (S_i(t_j))^2$$

the summation over j is limited only for $t_i - \Delta t < t_j < t_i + \Delta t$

Improvement of heat flux measurement

Time response improvement

- Thermocouple (TC) position
- High speed data logger

TC noise reduction

- Insulation amplifier
- Shield box
- Reference shot compensation

Noise reduction of DAQ system

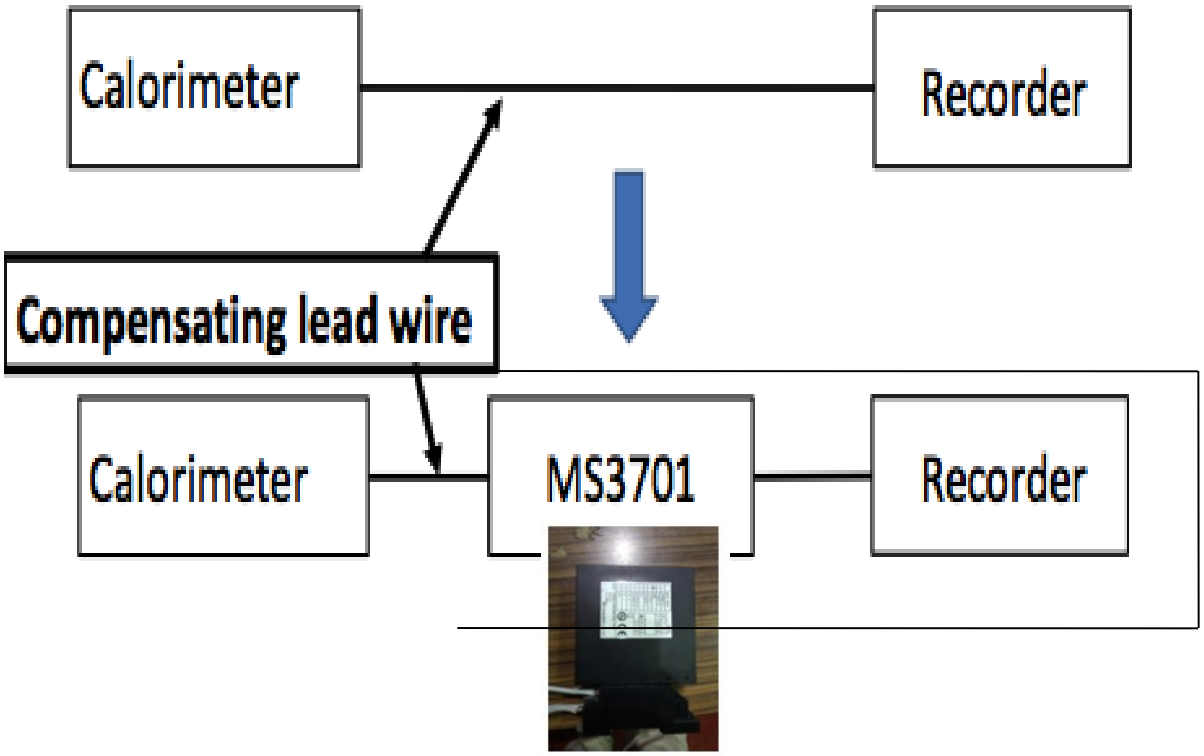

MS3701

In 2015 Fy, thermoelectric converter which is insulation amplifier for thermocouple was introduced. (MS3701)

Recorder (GL900)

Fast recorder(10 μs ~ 1 min)
2012

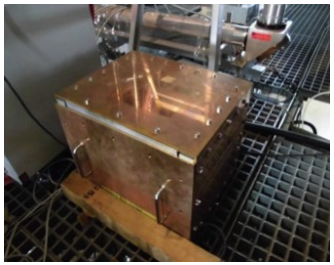

In 2016Fy, copper shield box was introduced and MS3701 and recorder were set in it.

Insulation amplifier effect

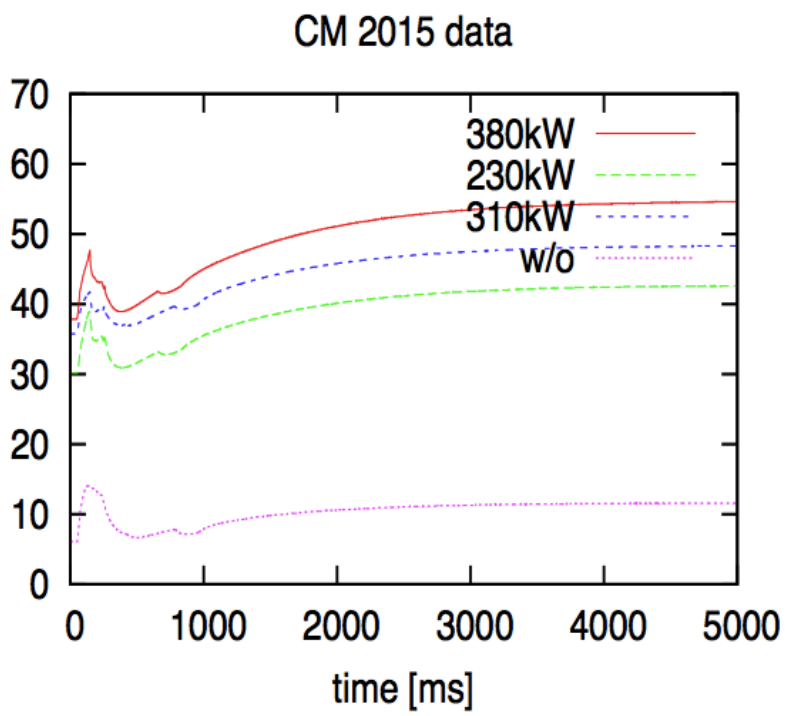

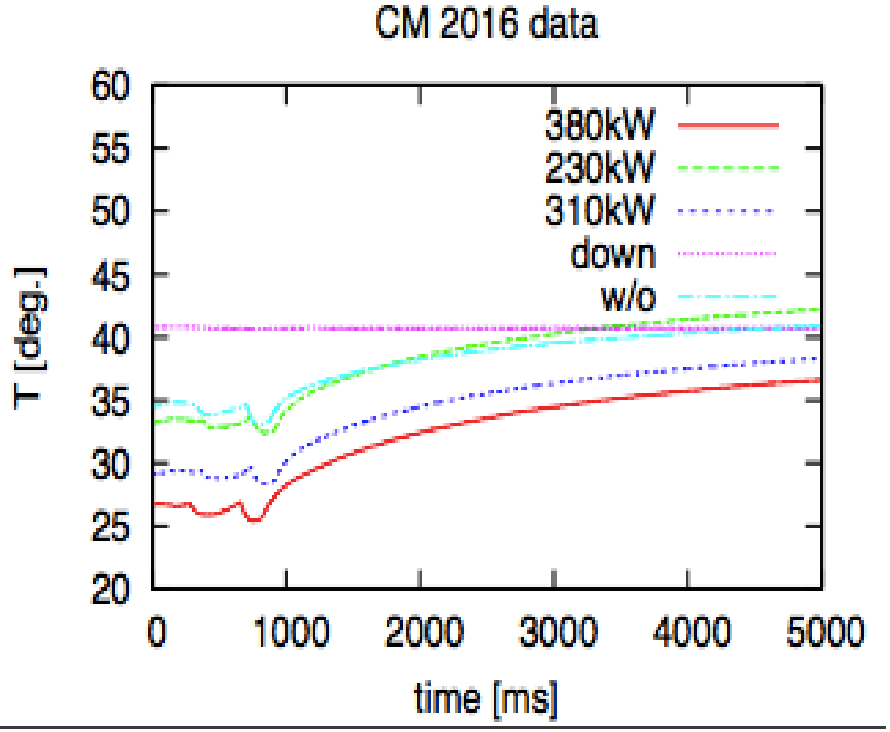

Although signal during plasma shot (50 ~ 250 ms) is apparently due to plasma heat flux, this is only noise from RF power source. Real plasma heat flux effect is temperature increment after discharge stop, whose peak is at 3 ~ 5 s.

Coil current

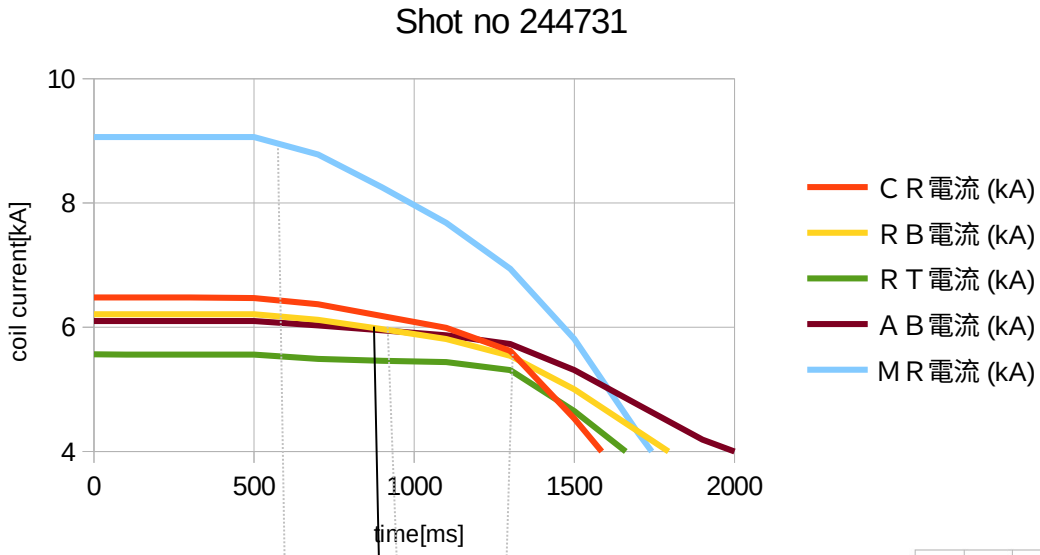

CM TC

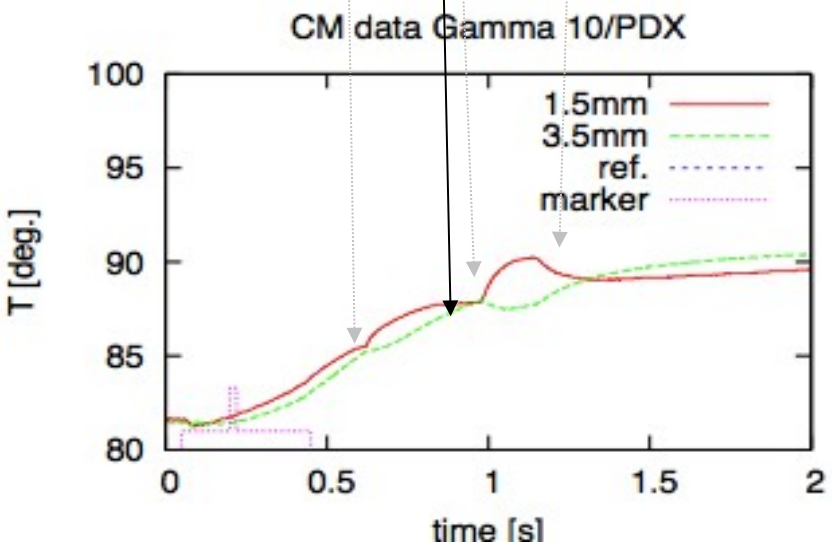

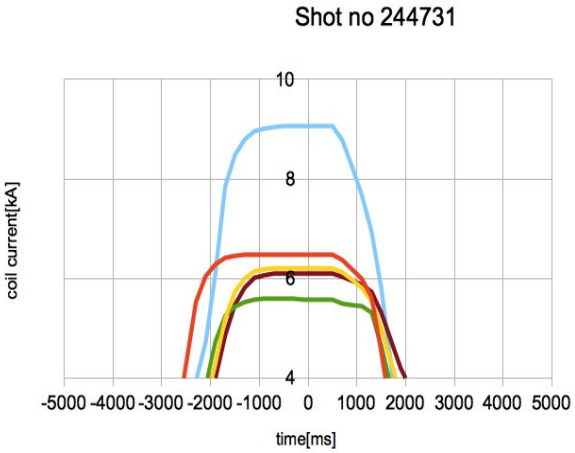

By Dr. Minami

TC signal noise compensation

During and just after discharge, there exist large noises in TC signal.
They come from RF power, magnetic field induction, ...

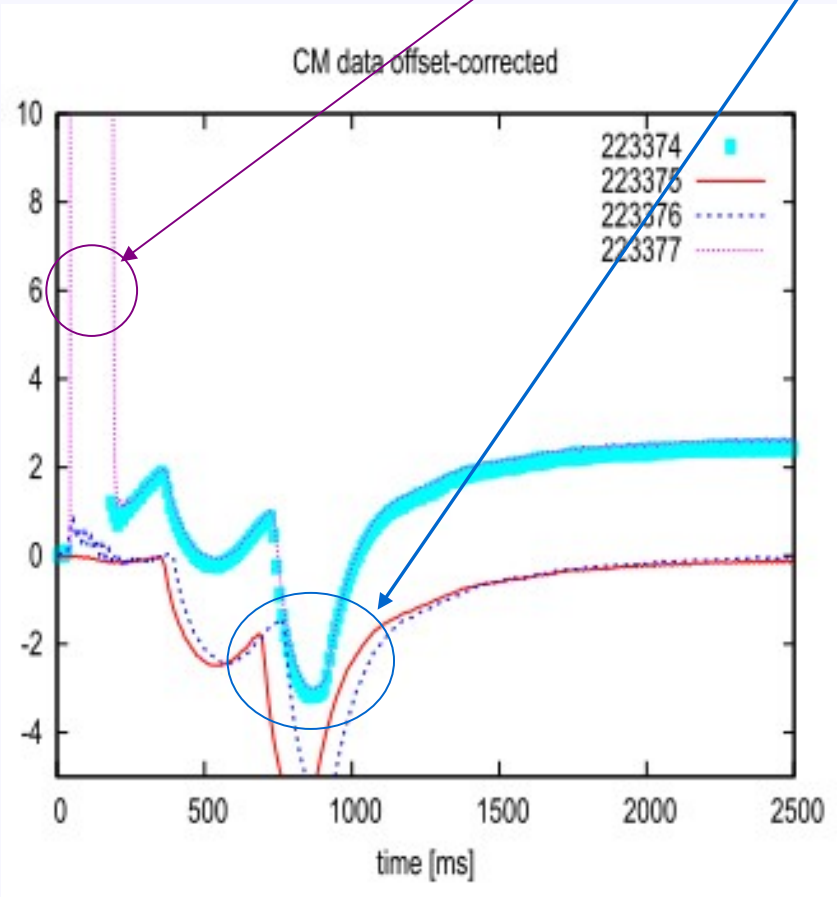

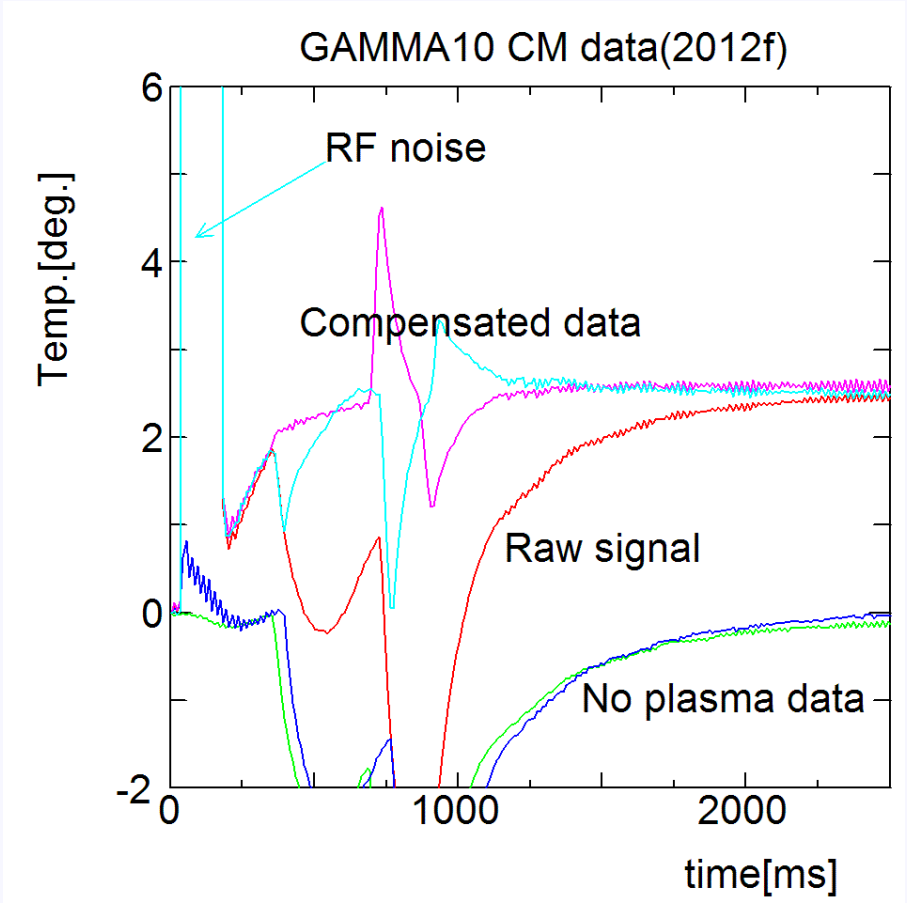

Noise at t=400-2000ms is well compensated with no plasma shot data.

Gradient method results(239195)

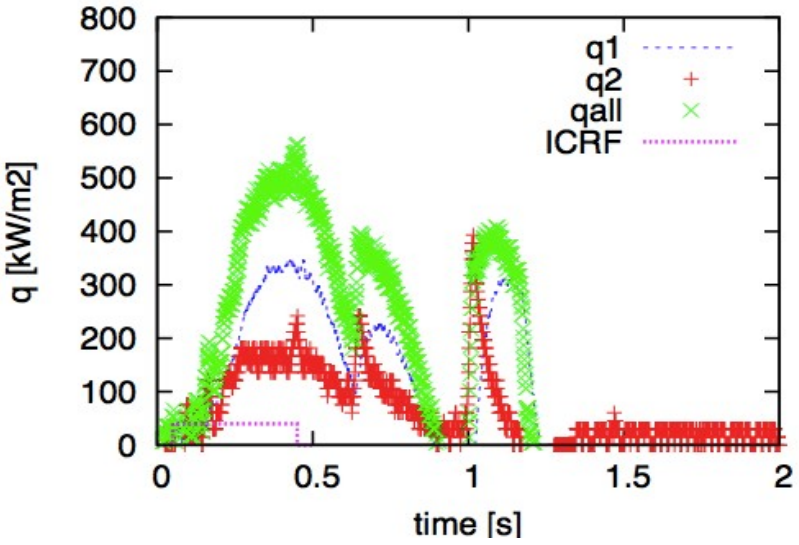

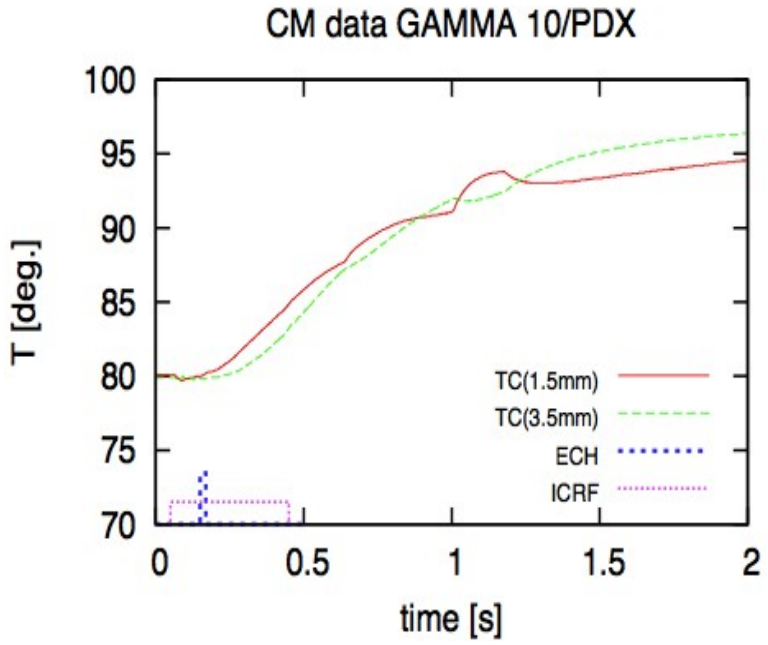

GAMMA 10/PDX movable calorimeter signal for shot # 239195.
ECH is applied at 150 – 169 ms to emulate ELM heat pulse.
Space gradient term q1 and time derivative term q2 are almost same for GAMMA 10/PDX plasma.
Heat flux after t = 600 ms is unrealistic. How about t < 600 ms ?

Pulse decompose method results(239195)

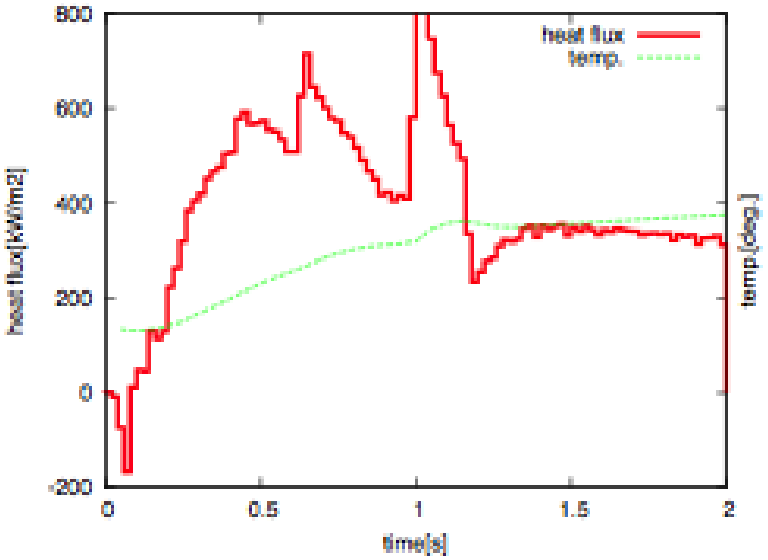

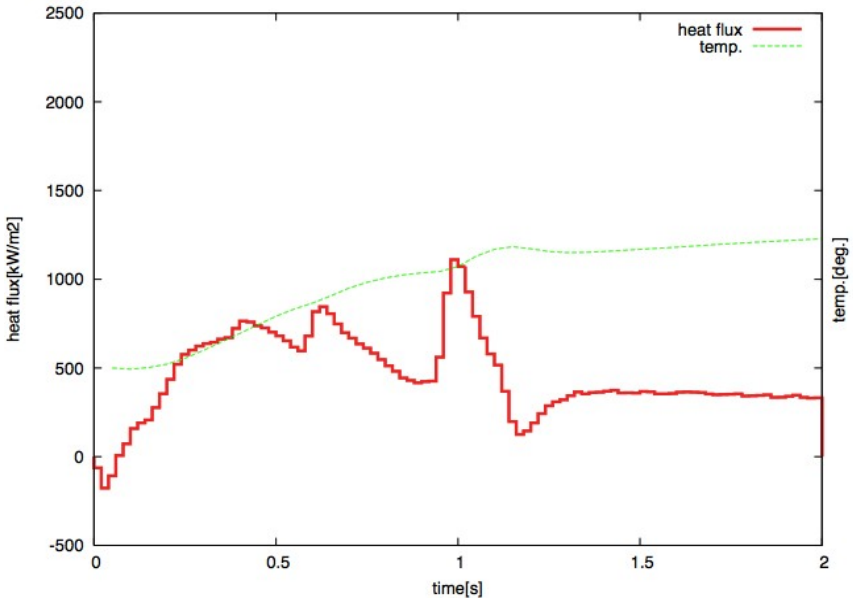

Model parameter such as delay time of the sensor or number of data in fitting is not theoretically optimized.
(right figure: delay time is 4 times larger, slow TC sensor.)
TC sheath may make its response slow.

Comparison of short pulse ECH

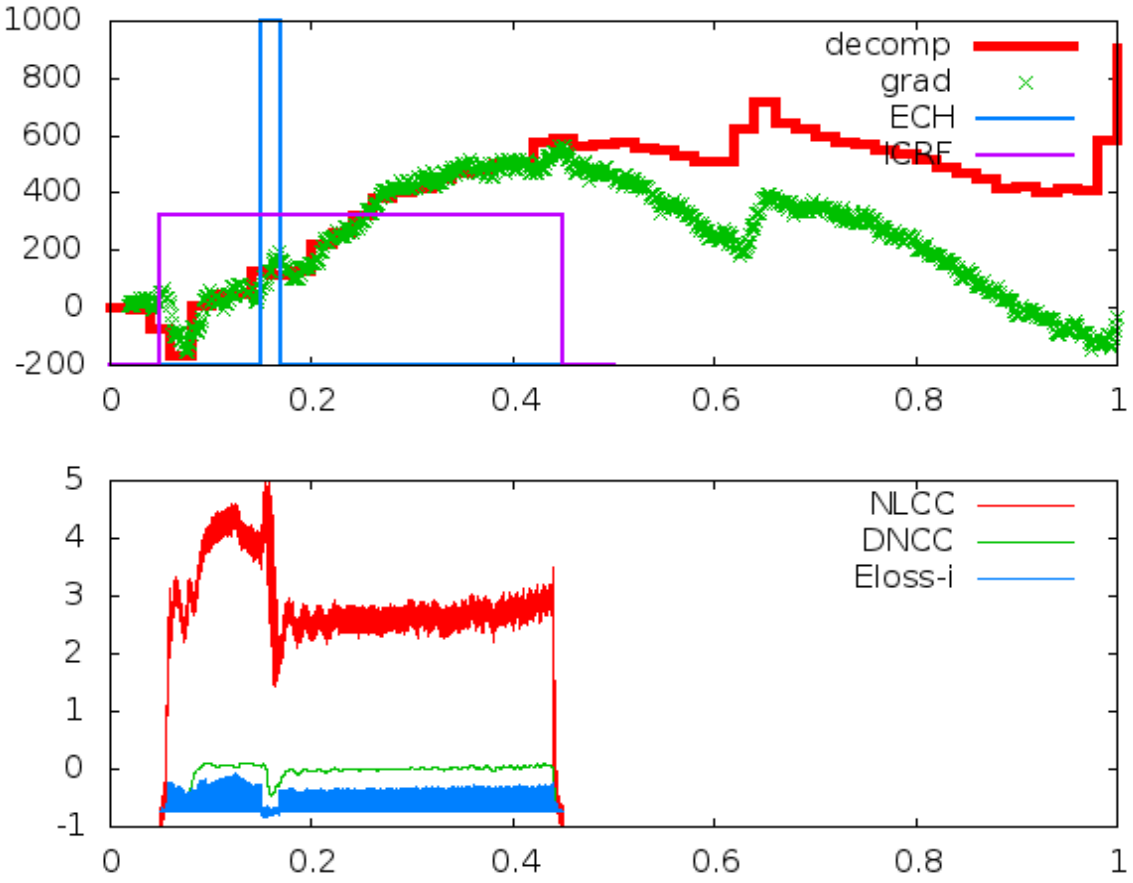

No clear heat flux pulse can not be reconstructed in present analysis.

Recently, we found another time delay in thermocouple system.(see Mr.Nhat Son)

Limitation of measurement

Temperature response of heat flux delays by order of thermal diffusion time and another delay of TC system(~0.010s and ~0.20s in GAMMA10/PDX experiment)

So fast change of heat flux can not be reproduced only with small size sensor(small thermal diffusion time).

TC system suffers many kind of electromagnetic noise. This demand to use filtering or averaging for TC data.

Heliotrons and LHD

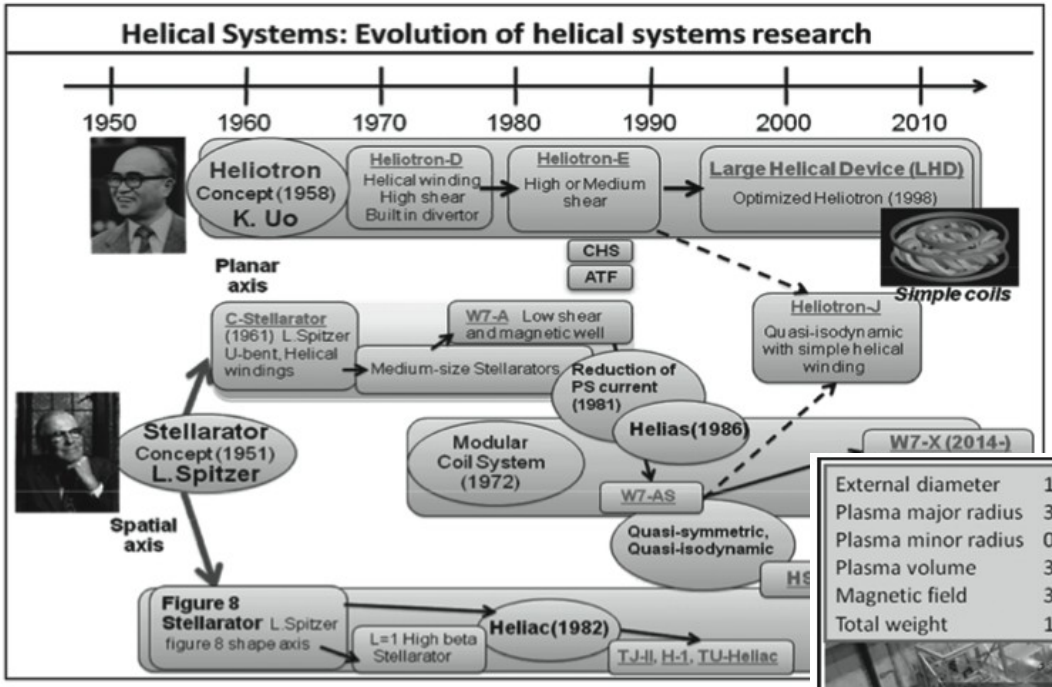

Heliotron is Japan-original concept, which was invented by Prof. Uo (Kyoto Univ.) and succeeded to Large Helical System (NIFS). LHD is currently largest fusion device in Japan.

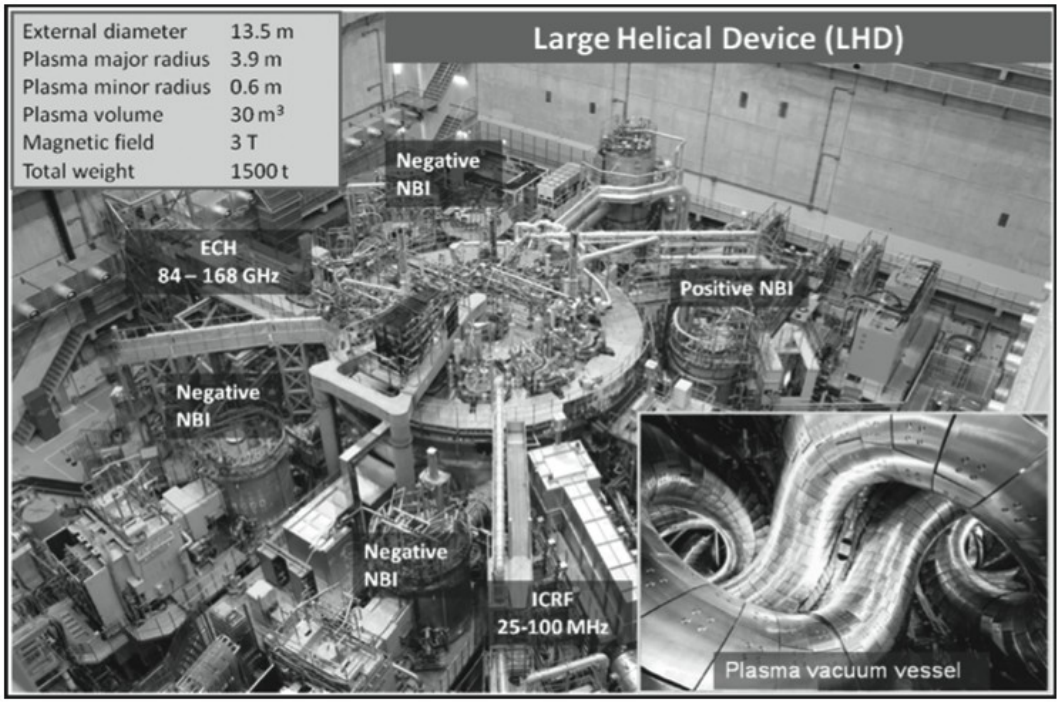

Journal of Plasma and Fusion Research
Vol.85, No.8
August 2009

HDLP for Large Helical Device

Thermal diffusion time is of the same order as discharge duration.
Probe temperature data is directly affected by the heat flux change.

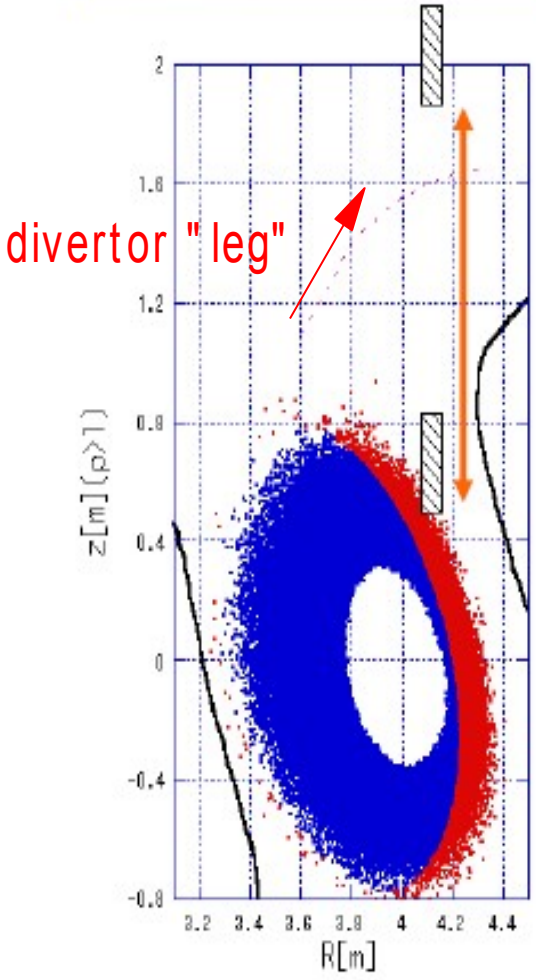

New channel is equipped for divertor leg measurement.

Spatial resolution: 1~6mm
Particle flux: from Iis
Electron temp.: from V-I data
Heat flux: this work

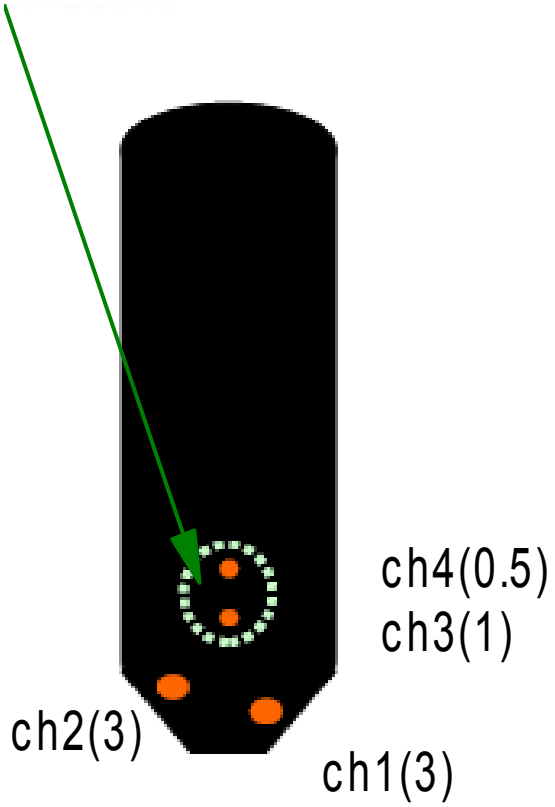

Detach plasma formation in LHD

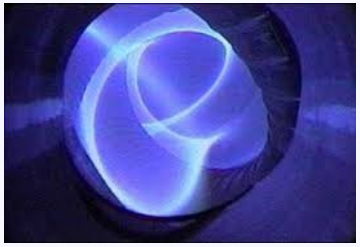

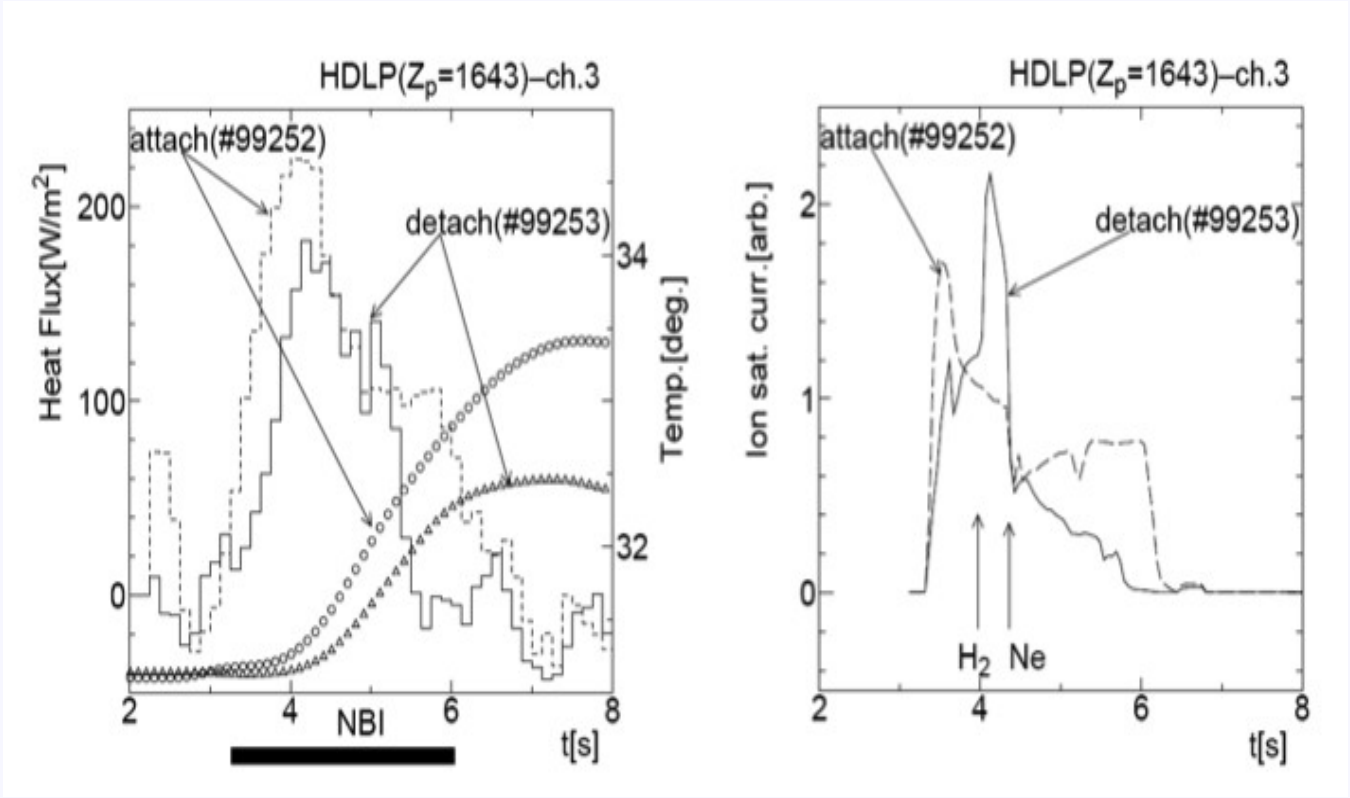

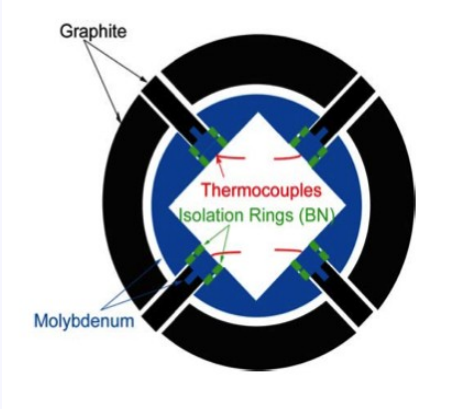

Hydrogen divertor plasma is terminated by contact with neon gas.
This heat flux control was monitored for the first time.

Edge plasma events

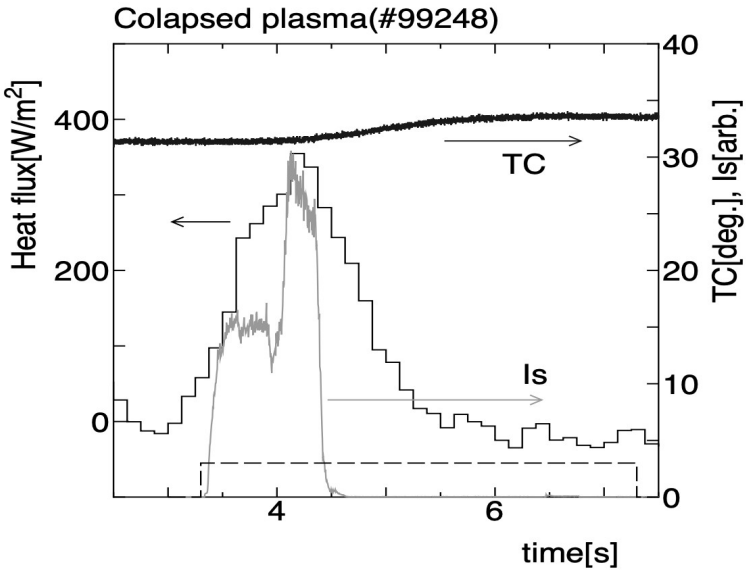

Radiation Coups

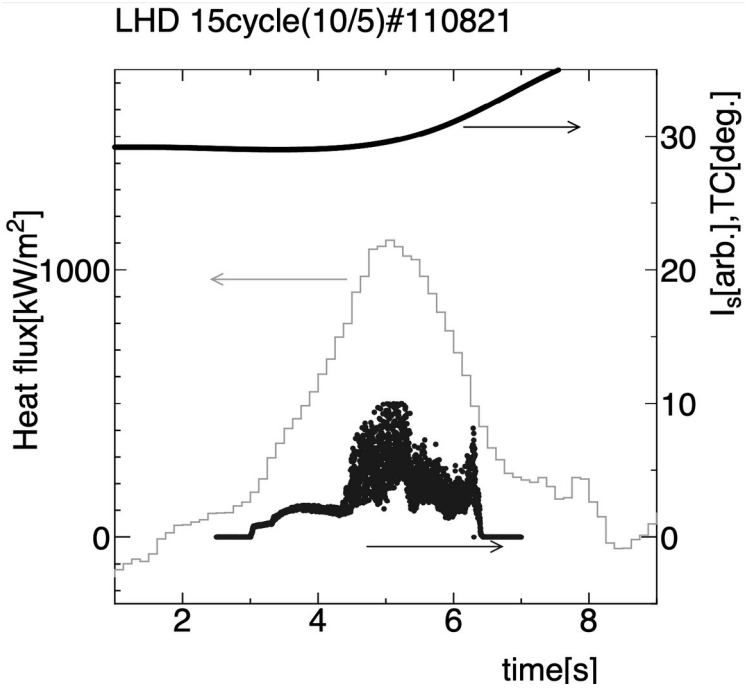

Non-diffusion transport, Blob

LHD NBI shine through power